

# Colloquium: Nonequilibrium effects in superconductors with a spin-splitting field

F. Sebastian Bergeret,<sup>1,2,\*</sup> Mikhail Silaev,<sup>3</sup> Pauli Virtanen,<sup>4</sup> and Tero T. Heikkilä<sup>3,†</sup>

<sup>1</sup>*Centro de Física de Materiales (CFM-MPC),  
Centro Mixto CSIC-UPV/EHU,  
Manuel de Lardizabal 4,  
E-20018 San Sebastian,  
Spain*

<sup>2</sup>*Donostia International Physics Center (DIPC),  
Manuel de Lardizabal 5,  
E-20018 San Sebastian,  
Spain*

<sup>3</sup>*University of Jyväskylä,  
Department of Physics and Nanoscience Center,  
P.O. Box 35 (YFL),  
FI-40014 University of Jyväskylä,  
Finland*

<sup>4</sup>*NEST, Istituto Nanoscienze-CNR and Scuola Normale Superiore, I-56127 Pisa,  
Italy*

We review the recent progress in understanding the properties of spin-split superconductors under non-equilibrium conditions. Recent experiments and theories demonstrate a rich variety of transport phenomena occurring in devices based on such materials that suggest direct applications in thermoelectricity, low-dissipative spintronics, radiation detection and sensing. We discuss different experimental situations and present a theoretical framework based on quantum kinetic equations. Within this framework we provide an accurate description of the non-equilibrium distribution of charge, spin and energy, which are the relevant non-equilibrium modes, in different hybrid structures. We also review experiments on spin-split superconductors and show how transport measurements reveal the properties of the non-equilibrium modes and their mutual coupling. We discuss in detail spin injection and diffusion and very large thermoelectric effects in spin-split superconductors.

## CONTENTS

I. Introduction	1	C. Spin Seebeck effect	18
II. Superconductor with an exchange field	4	D. Thermophase in a S(FI)S contact	18
A. Brief overview of the quasiclassical theory of diffusive superconductors	6	VI. Summary and Outlook	18
III. Nonequilibrium modes in spin-split superconductors	8	Acknowledgments	20
A. Description of nonequilibrium modes in superconductors with spin splitting	9	References	20
B. Accumulations in terms of the non-equilibrium modes	10	<b>I. INTRODUCTION</b>	
IV. Spin injection and diffusion in superconductors	11	Ferromagnetism and spin-singlet superconductivity are antagonist orders and hardly coexist in bulk materials. However, hybrid nanostructures allow for the possibility of combining the two phenomena via mutual proximity effects. The combination leads to the emergence of novel features not present in either system alone. We can make a distinction among those characteristics affecting the spectral properties of the materials, showing up when the probed systems are in equilibrium, and those related to nonequilibrium phenomena. The emphasis of our text is in the latter phenomena, especially related to steady-state currents or voltages applied across the structures.	
A. Detection of spin and charge imbalance: Non-local transport measurements	11	Both superconductors and ferromagnets are examples of electron systems with spontaneously broken symmetries, and thereby characterized by order parameters.	
B. Non-local conductance measurements in spin-split superconductors	12		
C. Spin Hanle effect	13		
D. Spin imbalance by ac excitation	14		
V. Thermoelectric effects	14		
A. Charge and heat currents at a spin-polarized interface to a spin-split superconductor	15		
B. Linear response: heat engine based on a superconductor/ferromagnet structure	15		

\* sebastian.bergeret@ehu.eus

† Tero.T.Heikkila@jyu.fi

The order parameter for a conventional spin singlet superconductor is the amplitude of (Cooper) pairing between electrons in states with opposite spins and momenta (Bardeen *et al.*, 1957). The presence of this complex pairing amplitude  $F$  leads to two characteristic features of conventional superconductivity (de Gennes, 1999; Tinkham, 1996): An equilibrium supercurrent that is proportional to the gradient of the phase of  $F$  and that can be excited without voltage, and to the quasiparticle spectrum exhibiting an energy gap proportional to the absolute value of  $F$ . The resulting density of states (DOS, Eq. (1) for  $h_{\text{eff}} = 0$ ) is strongly energy dependent and results into a non-linear nonequilibrium response of superconductors.

The main defining feature of ferromagnets is the broken spin-rotation symmetry into the direction of magnetization, and the associated exchange energy  $h$  that splits the spin up and down spectra. This also leads to a strong spin dependence (spin polarization) of the observables related to ferromagnets.

There are two mechanisms that prevent most of the ferromagnetic materials from becoming superconducting. One of them is the orbital effect due to the intrinsic magnetic field in ferromagnets. When this field exceeds a certain critical value, superconductivity is suppressed (Ginzburg, 1957). The second mechanism is the paramagnetic effect Chandrasekhar (1962); Clogston (1962); and Saint-James *et al.* (1969). This is due to the intrinsic exchange field of the ferromagnet that shows up as a splitting of the energy levels of spin-up and spin-down electrons and hence prevents the formation of Cooper pairs. We focus here on the regime where this spin-splitting field is present, but not yet too large to kill superconductivity.

In superconductors the spin-splitting field can be generated either due to the Zeeman effect in magnetic field or as a result of the exchange interaction between the electrons forming Cooper pairs and those which determine the magnetic order. Such fields can lead to drastic modifications of the ground state of a spin-singlet superconductor. The best-known example is the formation of the spatially inhomogeneous superconducting state predicted by Fulde and Ferrell (1964) and Larkin and Ovchinnikov (1965) and dubbed as FFLO. Although extensively studied in the literature, the FFLO phase only takes place in a narrow parameter window and therefore its experimental realization is challenging.

Other more robust phenomena related to the spin-splitting fields in superconductors have their origin in the quasiparticle spectrum modification. In the central panel of Fig. 1 we show the resulting spin-split density of states. This was first explored experimentally by Meservey *et al.* (1975, 1970) through the spin-valve effect in the superconductor/ferromagnet (Al/Ni) tunnel junctions (Fig. 1a). In these experiments the magnetic field was applied in the plane of a thin superconducting film, such that the paramagnetic effect domi-

ates. The spin-split DOS was utilized to determine the spin polarization of an adjacent ferromagnet (Meservey *et al.*, 1980; Meservey and Tedrow, 1994; Paraskevopoulos *et al.*, 1977; Tedrow and Meservey, 1971, 1973). The basis of this spin-valve effect is the spin-resolved tunneling into the superconductor with spin splitting, shown in Fig. 1a. This schematic picture illustrates how by properly tuning the voltage across the junction, the electronic transport is dominated by only one of the spin species. That results in peculiar asymmetric differential conductance curves  $dI/dV(V) \neq dI/dV(-V)$  observed in experiments and revealing the spin polarization. This idea has been used more recently to probe the spatially resolved spin polarization of different magnetic materials by means of scanning tunneling microscopy with spin-split superconducting tips (Eltschka *et al.*, 2014, 2015). Similar effects can also arise in thin superconducting films by the magnetic proximity effect from an adjacent ferromagnetic material (Tedrow *et al.*, 1986). In such a case, the spin splitting of the density of states can be observed for small magnetic fields or even at zero field, as discussed in Sec. II.

The combination of spin-splitting fields with strong spin-orbit interaction in superconducting nanowires has also raised considerable interest as a platform for realizing topological phases and Majorana fermions, with possible applications in topological quantum computation (Aasen *et al.*, 2016). Although these effects are beyond the focus of this review, the physics discussed below may help in understanding transport properties of the devices studied in that context.

Due to the different nature of their broken symmetry, combining superconductors (S) and ferromagnets (FM) in hybrid structures leads to a multitude of effects where magnetism affects superconductivity and vice versa. Some of these effects show up already in equilibrium properties, especially studied in the context of proximity effects in superconducting/metallic ferromagnet hybrids and reviewed for example by Buzdin (2005) and Bergeret *et al.* (2005). The latter usually focus on the unusual behavior of Cooper pairs leaking from a superconductor into a metallic ferromagnet generating, for example, oscillating pair wave functions analogous to the FFLO state (Buzdin *et al.*, 1982; Demler *et al.*, 1997) and long-range spin triplet correlations (Bergeret *et al.*, 2001b) induced by the coupling between the intrinsic exchange field of the ferromagnet and the leaked superconducting condensate (Bergeret *et al.*, 2001b). These effects manifest themselves in measurable equilibrium effects, such as the density of states and critical temperature oscillations in S/FM bilayers (Jiang *et al.*, 1996; Kontos *et al.*, 2001), triplet spin valve effects in the critical temperature of FM/S/FM structures (Singh *et al.*, 2015), and unusual Josephson effects in SC/FM/SC junctions (Ryazanov *et al.*, 2001; Singh *et al.*, 2016). Inversely, a magnetic proximity effect can arise when the triplet

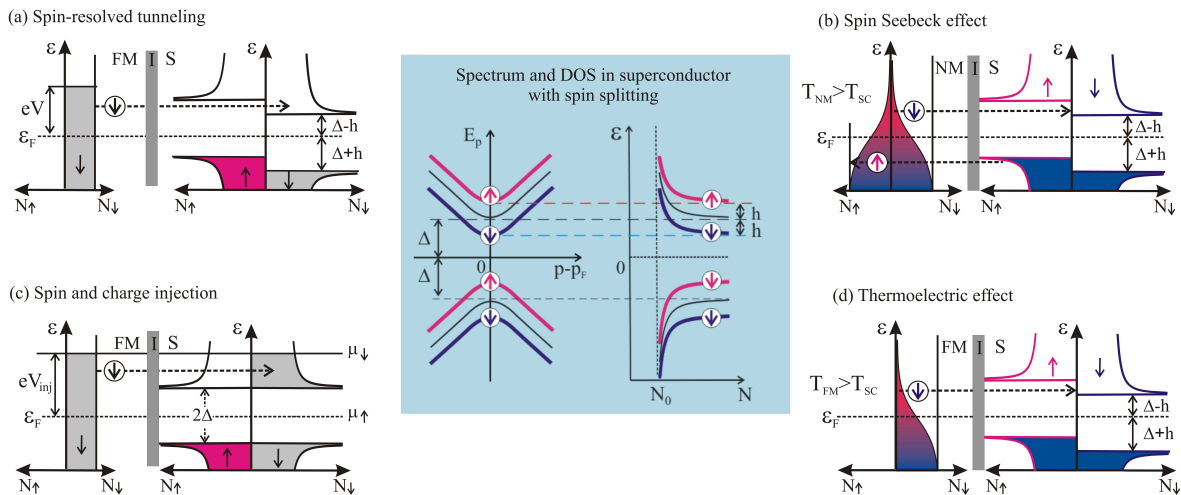


FIG. 1 Central panel: quasiparticle spectrum and density of states in a superconductor with spin splitting,  $N_0$  is the normal metal DOS. (a-d) Schematic pictures of various nonequilibrium phenomena occurring at normal metal/insulator/superconductor (NM/I/S) and ferromagnetic/insulator/superconductor (FM/I/S) interfaces discussed in this review. For clarity we show the limit of half-metallic FM with  $N_{\uparrow} = 0$ . (a) Spin-resolved tunneling from a ferromagnetic metal to a spin-split superconductor that leads to the spin valve effect, *i.e.*, the charge current in the parallel magnetic configuration is different from that in the anti-parallel one. (c) Creation of spin and charge accumulation in the voltage biased FM/S junction. (b,d) Schematic picture of thermally excited currents in NM/S and FM/S junctions with a spin-split superconductor. (b) Spin Seebeck effect in NM/S junction: A pure spin current is generated by the temperature bias between a spin-split superconductor at temperature  $T_{SC}$  and a normal metal at temperature  $T_{NM} > T_{SC}$ . (d) Thermoelectric effect in a FM/I/S junction: Here the spin current is partially converted to the charge current due to the spin-dependent density of states in the ferromagnet.

pairs, created in the FM region, leak back into the superconductor in a FM/S metallic bilayer, generating a non-vanishing magnetic moment in the SC within a coherence length  $\xi_s$  from the SM/FM interface (Bergeret *et al.*, 2004).

In contrast to these equilibrium proximity effects, here we focus on nonequilibrium properties of a superconducting material with a built-in spin-splitting field. The interest in studying such systems has been intensified recently due to the technological advances which allow for a controllable generation of spin splitting in thin superconducting films either by applying an external in-plane magnetic field (Hübler *et al.*, 2012; Quay *et al.*, 2013) or by an adjacent ferromagnetic insulator. Structures with insulating FMs avoid the proximity effect suppressing superconductivity. Such nonequilibrium properties are studied by applying currents or voltages across the structures. The focus of our Colloquium is on steady-state nonequilibrium effects with time independent driving fields, but we also mention works studying alternating current (ac) responses.

Often the nonequilibrium effects can survive to much higher distances than  $\xi_s$ , as their decay scales are determined via the various inelastic and spin-flip scattering lengths. Moreover, they can be studied at a weak tunneling contact to ferromagnets, making the analysis in some cases more straightforward than in proximity experiments. Nonequilibrium properties are related to the deviation of the electron distribution function from its

equilibrium form, which leads to a nonequilibrium distribution (imbalance) of charge, energy or spin degrees of freedom. We refer to these different types of deviations from equilibrium as nonequilibrium modes.<sup>1</sup> Specifically, we explore the coupling between these modes in superconductors with a spin-splitting field, and discuss unusually strong thermoelectric response and long-range spin signals.

The above mentioned ability to characterize the spin polarized Fermi surface of metallic magnets with the help of spin-split superconductors has a direct connection with spintronics, and in particular with the search for spin valves with larger efficiencies than in the structures exhibiting large magnetoresistance (Baibich *et al.*, 1988; Binasch *et al.*, 1989; Moodera *et al.*, 1995). Indeed, a superconductor with a spin-splitting field has also an intrinsic energy dependent spin polarization around the Fermi level. This allows for studying different spintronic effects in a setting of a controllable non-linearity arising from the superconducting gap. Some of these effects are schematically shown in Fig. 1. This review explains those phenomena in detail.

<sup>1</sup> The term "mode" here refers to the changes of the electron distribution function with respect to its equilibrium form. It should be distinguished from collective modes such as the Carlson and Goldman (1973) or the amplitude mode (Higgs, 1964) that affect the response of superconductors at temperatures close to the critical temperature or at high frequencies.

In normal metals and superconductors a spin accumulation, or spin imbalance, can be created by injection of a charge current from a ferromagnetic electrode (Gu *et al.*, 2002; Jedema *et al.*, 2001; Johnson, 1994; Johnson and Silsbee, 1985; Poli *et al.*, 2008; Shin *et al.*, 2005; van Son *et al.*, 1987; Takahashi and Maekawa, 2003). This state is characterized by the excess population in one of the spin subbands, determined by the balance between spin injection and relaxation or spin diffusion rates. In normal metals the nonequilibrium spin imbalance decays due to spin-flip scattering at typical distances of several hundreds of nanometers. In the superconducting state, at low temperatures  $k_B T \ll \Delta$  the injection of any amount of carriers just above the energy gap shifts the chemical potential of quasiparticles rather strongly due to the large amount of quasiparticles at the gap edge [Fig. 1(c)]. This leads to a strong spin signal in SF junctions (Poli *et al.*, 2008; Takahashi and Maekawa, 2003).

The spin relaxation length in normal metals depends only weakly on the temperature  $T$ . In the superconducting state, however, the scattering length is drastically modified with  $T$ . According to the first theory and experiments on spin injection in superconductors, the spin relaxation length was found to be reduced compared to the normal state (Morten *et al.*, 2004; Poli *et al.*, 2008). However, subsequent experiments showed, contrary to expectations, an increase of the spin decay length (Hübler *et al.*, 2012; Quay *et al.*, 2013). It is now understood that these findings can only be explained by taking into account the spin-splitting field inside the superconductor (Bobkova and Bobkov, 2015, 2016; Krishtop *et al.*, 2015; Silaev *et al.*, 2015a). Due to this field, as shown in Sec. III.B, it is necessary to take into account four types of nonequilibrium modes describing spin, charge, energy, and spin-energy imbalances. These modes provide the natural generalization of the charge and energy imbalances introduced by Schmid and Schön (1975). In Sec. IV we show how the spin-splitting field couples pairwise these modes: charge to spin energy and spin to energy. Such a coupling leads to striking effects. For example, the coupling between the spin and energy modes leads to the long-range spin-accumulation observed in the experiments by Hübler *et al.* (2012) and Quay *et al.* (2013). As we show in Sec. IV this long-range effect is related to the fact that the energy mode can only relax via inelastic processes which at low temperatures are rare.

The coupling between different modes shows up also in tunnel contacts with spin-split superconductors. Because the spin-splitting field shifts the spin-resolved DOS away from the chemical potential of the superconductor, the system exhibits a strong spin-dependent electron-hole asymmetry. The spin-averaged density of states is still electron-hole symmetric, and therefore does not violate fundamental symmetries of the (quasiclassical) superconducting state. This spin-resolved electron-hole asymmetry leads to a large *spin Seebeck effect* shown schemati-

cally in Fig. 1b and discussed in Sec. V.C. A temperature difference across a tunneling interface between a normal metal and a spin-split superconductor drives a pure spin current between the electrodes, without transport of charge. If one of the electrodes is small so that the spin injection rate is large or comparable to the rate for spin relaxation, a spin accumulation forms in this electrode.

However, it was noticed in several recent works (Kalenkov *et al.*, 2012; Machon *et al.*, 2013, 2014; Ozaeta *et al.*, 2014) that in certain situations the relevant observables are not spin-averaged, resulting in an effective electron-hole asymmetry showing up also in the charge current. The spin components are weighted differently in a setup consisting of the spin-filter junction connected to the spin-split superconductor (Ozaeta *et al.*, 2014), shown schematically in Fig. 1d. As a result of this effective electron-hole symmetry breaking, the system exhibits a very large thermoelectric effect. This is discussed in Sec. V.

The main body of the review is organized as follows. In Sec. II we describe spin-split superconductors and give an overview of the quasiclassical theory that can be used for describing both their equilibrium and nonequilibrium properties. In Sec. III we describe the nonequilibrium modes in superconducting systems driven out of equilibrium in terms of the quasiclassical formalism. Section IV focuses on the spin injection and diffusion in superconducting systems, and reviews experiments performed to detect spin and charge imbalance in superconductors with and without spin-splitting. In Sec. V we describe the giant thermoelectric response of a system exhibiting spin-polarized tunneling into a superconductor with a spin-splitting field. Finally, we present our conclusions and an outlook on possible future developments in the field in Sec. VI. A longer version of this review, along with comprehensive technical detail, can be found at (Bergeret *et al.*, 2017).

## II. SUPERCONDUCTOR WITH AN EXCHANGE FIELD

The main focus of this colloquium is on superconductors with a spin-split density of states (DOS). As discussed in the introduction such a splitting can originate either by an external magnetic field (Meservey *et al.*, 1970) or by the exchange field induced by an adjacent ferromagnetic insulator (Tedrow *et al.*, 1986). The split DOS was observed in spectroscopy experiments (Hao *et al.*, 1990; Meservey *et al.*, 1980, 1970; Paraskevopoulos *et al.*, 1977; Tedrow and Meservey, 1971; Xiong *et al.*, 2011).

Formally, the normalized DOS of a spin-split Bardeen-Cooper-Schrieffer (BCS) superconductor is expressed as

the sum of the DOS of each spin species,  $N = N_{\uparrow} + N_{\downarrow}$ ,

$$N = \frac{1}{2} \text{Re} \frac{\varepsilon + h_{\text{eff}}}{\sqrt{(\varepsilon + h_{\text{eff}})^2 - \Delta^2}} + \frac{1}{2} \text{Re} \frac{\varepsilon - h_{\text{eff}}}{\sqrt{(\varepsilon - h_{\text{eff}})^2 - \Delta^2}}, \quad (1)$$

where  $\pm h_{\text{eff}}$  is the effective spin-splitting field. Equation (1) is a simplified description because it does not take into account the effect of magnetic impurities or spin-orbit coupling (SOC) (Meservey and Tedrow, 1994) discussed below. Often inelastic processes are described by  $\varepsilon \mapsto \varepsilon + i\Gamma$ , where  $\Gamma$  is the Dynes *et al.* (1984) parameter.

In the case when the exchange field is induced by an adjacent ferromagnetic insulator (FI) there is no need of applying an external magnetic field (Hao *et al.*, 1990; Moodera *et al.*, 2007; Senapati *et al.*, 2011; Tedrow *et al.*, 1986; Wolf *et al.*, 2014b; Xiong *et al.*, 2011). Microscopically, the spin splitting originates from the exchange interaction between conduction electrons and the magnetic moments of the FI localized at the S/FI interface (Izyumov *et al.*, 2002; Khusainov, 1996; Tokuyasu *et al.*, 1988). The ferromagnetic ordering in the FI is due to a direct exchange coupling between the localized magnetic moments. In usual FIs the direct coupling is strong enough that one can assume that the magnetic configuration of the FI is only weakly affected by the superconducting state (Bergeret *et al.*, 2000; Buzdin and Bulaevskii, 1988).

The modification of the DOS is non-local and survives over distances away from the FI/S interface of the order of the coherence length  $\xi_s$  (Bergeret *et al.*, 2004; Tokuyasu *et al.*, 1988). If the thickness  $d$  of the S film is much smaller than  $\xi_s$ , the spin splitting can be assumed as homogeneous across the film. Thus the density of states can be approximated by Eq. (1) with an effective exchange field  $\mathbf{h}_{\text{eff}} \approx J_{\text{ex}} \langle \mathbf{S}_{\mathbf{r}} \rangle a/d$  (de Gennes, 1966a; Khusainov, 1996; Tokuyasu *et al.*, 1988), where  $a$  is the characteristic distance between the localized spins,  $J_{\text{ex}}$  is the exchange coupling between conduction electrons and localized moments, and  $\langle \mathbf{S}_{\mathbf{r}} \rangle$  is the average of the latter.

In Fig. 2 we show an example of the measured differential conductance of an EuS/Al/Al<sub>2</sub>O<sub>3</sub>/Al junction. The Al layer adjacent to the EuS has a spin-split density of states that shows up as the splitting peaks (bright stripes in the figure) in  $dI/dV$ . Even at zero applied magnetic field the splitting is nonzero. The magnetization reversal of EuS at  $H_c \approx -18.5$  mT manifests as a discontinuity of the conductance peaks (Strambini *et al.*, 2017). As a first approach the DOS inferred from Fig. 2 can be well described by the expression (1).

The advantage of using a FI instead of an external magnetic field is that one avoids the depairing effects and all complications caused by the need to apply magnetic fields in superconducting devices. Moreover, because the electrons of the superconductor cannot propagate into the FI, superconducting properties are only modified by the induced spin-splitting field at the S/FI interface, and not by the leakage of Cooper pairs into the FI as would

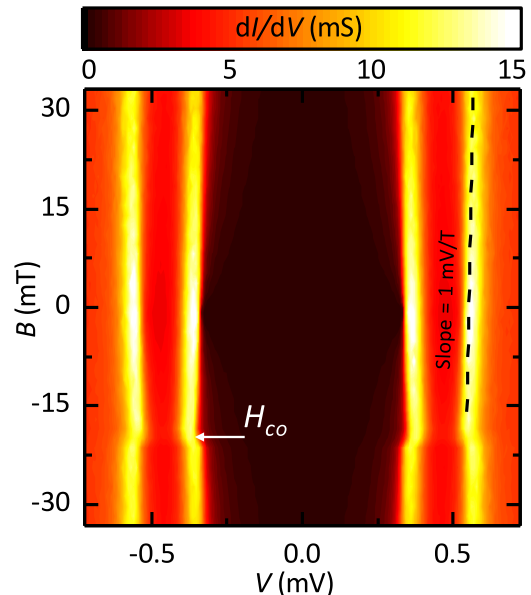


FIG. 2 Color plot of measured differential conductance,  $dI/dV$  of a EuS/Al/Al<sub>2</sub>O<sub>3</sub>/Al junction as a function of the applied voltage and external magnetic field.  $H_{co}$  denotes the coercive field of the EuS layer when the magnetization switches. Figure adapted from the work by Strambini *et al.* (2017)

happen in the case of metallic ferromagnets. In addition, FIs can also be used as spin-filter barriers (Moodera *et al.*, 2007), in some cases with a very high spin-filtering efficiency, and therefore they play a crucial role for different applications as discussed below.

In Table I we show a list of FI/S combinations and the reported induced exchange splittings and spin-filter efficiencies (barrier spin polarizations).

The paramagnetic effect, that leads to the spin-splitting, is modified by spin relaxation and orbital depairing. In their absence the superconductivity survives the spin-splitting field up to the Chandrasekhar-Clogston limit (Chandrasekhar, 1962; Clogston, 1962)  $h = \Delta_0/\sqrt{2}$ , where  $\Delta_0$  is the order parameter at zero-field and zero-temperature. At this field the system experiences a first-order phase transition into the normal state when the order parameter changes abruptly from  $\Delta_0$  to zero. This picture changes qualitatively due the presence of magnetic impurities and spin-orbit scattering. Even at  $T = 0$  and  $h = 0$  the spin-flip processes induced by magnetic impurities result in the pair breaking effect closing the energy gap (Abrikosov and Gor'kov, 1960a) at  $\tau_{sf}\Delta_0 = 3/4$  and suppresses superconductivity completely at a certain critical value of the spin-flip time  $\tau_{sf}$ . For values of  $\tau_{sf}$  larger than the critical one the phase transition switches from the first to the second order at (Bruno and Schwartz, 1973)  $\tau_{sf}\Delta_0 = 0.461$  and the gapless state appears at a certain value of  $h(\tau_{sf})$  (see Fig. 3a).

TABLE I Magnetic properties of different ferromagnetic insulator-superconductor junctions used in experiments. Middle column shows the spin-filter efficiency characterized by the polarization  $P = (G_{\uparrow} - G_{\downarrow}) / (G_{\uparrow} + G_{\downarrow})$  of the FI barrier (red) with normal-state conductance  $G_{\sigma}$  for spin  $\sigma$ . The exchange splittings measured in the superconductor (blue) are listed in the right column. The data is extracted from <sup>1</sup> (Tedrow *et al.*, 1986); <sup>2</sup> (Mooodera *et al.*, 1988); <sup>3</sup> (Hao *et al.*, 1990); <sup>4</sup> (Mooodera *et al.*, 1993); <sup>5</sup> (Senapati *et al.*, 2011); <sup>6</sup> (Pal and Blamire, 2015). Note that  $\mu_B \cdot 1 \text{ T} = 58 \mu\text{eV} \cong 670 \text{ mK}$ .

Material Combination	Barrier polarization	Exchange Splitting (applied field)
EuO/Al/AlO <sub>3</sub> /Al <sup>1</sup>	no spin-filter barrier	1 T (0.1 T)-1.73 T(0.4 T)
Au/ EuS/Al <sup>2</sup>	0.8	1.6 T (0 T)
Al/ EuS/Al <sup>3</sup>	0.6-0.85	1.9-2.6 T (0T)
Ag/ EuSe/Al <sup>4</sup>	> 0.97	none at zero field
EuSe/Al/AlO <sub>3</sub> /Ag <sup>4</sup>	no spin-filter barrier	4 T (0.6 T)
NbN/ GdN/NbN <sup>5</sup>	0.75	
NbN/ GdN/TiN <sup>6</sup>	0.97	1.4 T (0T)

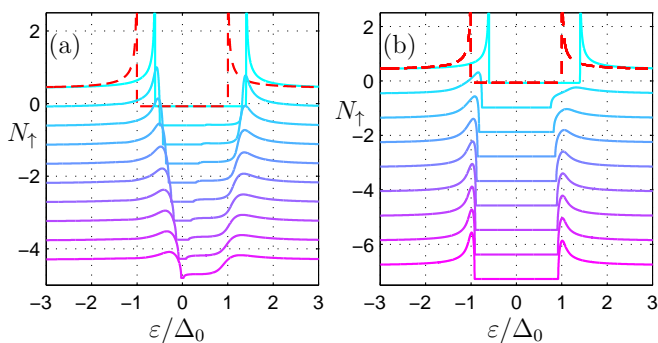


FIG. 3 Calculated density of states of a thin superconducting film at  $T \rightarrow 0$ . We only show the DOS for one of the spin species,  $N_{\uparrow}$ . Shown by dashed red lines is the DOS in the absence of relaxation  $\tau_{sn} = 1/(\tau_{sf}^{-1} + \tau_{so}^{-1}) = \infty$  and zero exchange field  $h = 0$  which corresponds to a gap  $\Delta_0$ . Other curves are plotted for  $h = 0.4\Delta_0$  and different spin relaxation rates. (a) Spin-flip relaxation  $\beta = (\tau_{so} - \tau_{sf}) / (\tau_{so} + \tau_{sf}) = 1$ , curves from top to bottom correspond to an increasing  $(\tau_{sn}\Delta_0)^{-1}$ , varying equidistantly from 0 by 0.04 steps. (b) Spin-orbit relaxation  $\beta = -1$ , curves from top to bottom correspond to an increasing  $(\tau_{sn}\Delta_0)^{-1}$ , varying equidistantly from 0 by steps of 3.4. For clarity the curves are shifted along the vertical axis.

Contrary to the spin-flip processes, the spin-orbit scattering alone does not have any effect on the superconducting state. However, in combination with  $h \neq 0$  it tends to smear out the spin-split DOS singularities provided the spin-orbit relaxation time,  $\tau_{so}$ , is not very short (see Fig. 3b). At short relaxation times  $\tau_{so} \ll \Gamma/\Delta^2$ , where  $\Gamma$  is the depairing parameter (Dynes *et al.*, 1984) the effect of spin splitting is eliminated and the usual BCS density of states is recovered (see Fig. 3b). Therefore in this case the critical spin-splitting field is strongly increased above the Chandrasekhar-Clogston limit (Bruno and Schwartz, 1973).

Besides broadening of the DOS singularities, the spin-orbit and spin-flip relaxation processes have an important effect on the paramagnetic spin susceptibility of the

superconductor as it becomes non-vanishing even in the zero-temperature limit (Abrikosov and Gor'kov, 1960b; Bruno and Schwartz, 1973; Yosida, 1958). The static spin susceptibility characterizes the paramagnetic response of the superconductor to an external magnetic field. In a usual normal metal the Zeeman field produces the same magnetization as a spin-dependent chemical potential shift  $\delta\mu$  of the same magnitude when the distribution functions in different spin subbands are given by  $f_{\uparrow}(E) = f_0(E + \delta\mu)$  and  $f_{\downarrow}(E) = f_0(E - \delta\mu)$ . This is different in superconductors where the paramagnetic susceptibility is determined by both the spin-polarized quasiparticles and the emergent spin-triplet superconducting correlations (Abrikosov and Gor'kov, 1960b, 1962). On the other hand, the non-equilibrium spin modes as systematically described in Sec. III are determined only by the quasiparticle contribution.

In the next sections we review the transport properties of diffusive hybrid structures with spin-split superconductors by contrasting existing theories and experiments. For this sake, in the next section we briefly introduce the quasiclassical Green's function formalism for superconductors in the presence of spin-dependent fields and spin-polarised interfaces. It is in our opinion the most suitable formalism for the description of diffusive hybrid structures.

### A. Brief overview of the quasiclassical theory of diffusive superconductors

Quasiclassical Keldysh Green's function technique is a useful and well-established way to describe transport and nonequilibrium properties of good metals, where the relevant physical length scales affecting different observables are long compared to the Fermi wave length  $\lambda_F$ , and where in particular disorder plays a major role. Several reviews explain this technique for various applications (Belzig *et al.*, 1999; Bergeret *et al.*, 2005). Here we just outline the main features relevant for spin-split

superconductors. Briefly, the Keldysh Green's functions (GFs),  $\check{G}(\mathbf{r}, \mathbf{r}'; \mathbf{t}, \mathbf{t}')$  are two-point correlation functions which depend on two coordinates and two times. Here the "check"  $\check{G}$  denotes GFs that live in a structure formed by the direct product of Keldysh, spin and Nambu spaces. The equation of motion for  $\check{G}$  can be written as a kinetic-like equation for the Wigner transformed GF,  $\check{G}(\mathbf{R}, \mathbf{p})$ , where  $\mathbf{R}$  and  $\mathbf{p}$  are the center of mass coordinate and  $\mathbf{p}$  the momentum after Fourier transformation with respect to the relative component. A significant simplification can be done in the case of metals by noticing that the Green's functions are peaked at the Fermi level. This allows for an integration of the equations over the quasiparticle energy, related to the magnitude of  $\mathbf{p}$ . This procedure leads to the quasiclassical GFs,  $\check{g}(\mathbf{R}, \mathbf{n})$ , which only depend on the direction of the momentum at the Fermi level and on two times in the case of non-stationary problems, or only on a single energy  $\varepsilon$  in the stationary case. These functions obey the Eilenberger (1968) equation. One of the advantages of using the quasiclassical GFs is that in the normal state, the spectral part is trivial, *i.e.*, the retarded and advanced GFs are energy independent. All transport information of the normal metal is encoded in the quasiclassical Wigner distribution function  $\hat{f}(\mathbf{R}, \mathbf{n})$  and quasiclassical equation for it resembles the classical Boltzmann equation (Langenberg and Larkin, 1986).

In contrast, the superconducting case distinguishes itself by a non-trivial spectrum, and therefore requires taking into account the full Keldysh structure of the GFs, *i.e.*

$$\check{g} = \begin{pmatrix} \hat{g}^R & \hat{g}^K \\ 0 & \hat{g}^A \end{pmatrix}. \quad (2)$$

This GF satisfies the normalization condition (Eilenberger, 1968)

$$\check{g}^2 = \check{1}. \quad (3)$$

In the diffusive limit the elastic mean free path  $l$  due to scattering at non-magnetic impurities is much smaller than any other length involved in the problem except  $\lambda_F$ . Within this limit the Eilenberger equation can be reduced to a diffusive-like equation, in the same way as the Boltzmann equation is simplified in the diffusive limit. This quasiclassical diffusion equation for superconductors is the Usadel (1970) equation (we set  $\hbar = k_B = 1$ )

$$D\nabla \cdot (\check{g}\nabla\check{g}) + [i\varepsilon\tau_3 - i\mathbf{h} \cdot \boldsymbol{\sigma}\tau_3 - \check{\Delta} - \check{\Sigma}, \check{g}] = 0. \quad (4)$$

Here  $D$  is the diffusion coefficient,  $\check{g}(\mathbf{r}, \varepsilon)$  is the isotropic (momentum independent) quasiclassical GF,  $\mathbf{h}$  the spin-splitting field either generated by an external field or by the magnetic proximity effect in a FI/S junction, and  $\check{\Delta} = \Delta e^{i\varphi\tau_3}\tau_1$  depends on the superconducting order parameter  $\Delta$  that has to be determined self-consistently. Here  $\tau_i$  and  $\sigma_i$  are Pauli spin matrices in Nambu and spin

space, respectively. The self-energy  $\check{\Sigma}$  in Eq. (4) describes different scattering processes, such as elastic spin-flip or spin-orbit scattering,  $\check{\Sigma}_{el}$  and inelastic electron-phonon and electron-electron scattering,  $\check{\Sigma}_{in}$ .

Equation (4) is central in the description of diffusive superconducting structures. Whereas the spectral properties can be obtained by solving the retarded (R) and advanced (A) components of this equation, nonequilibrium properties are described by the kinetic equation obtained by taking the Keldysh (K) component of Eq. (4). This can be compactly written as

$$\nabla_k j_{kb}^a = H^{ab} + R^{ab} + I_{coll}^{ab}, \quad (5)$$

where we introduce the spectral current tensor  $j_{kb}^a$ ,

$$j_{kb}^a = \frac{1}{8} \text{Tr} \tau_b \sigma_a (\check{g} \nabla_k \check{g})^K. \quad (6)$$

The different current density components (charge, spin, energy, spin-energy) can be obtained from Eq (6). For example, the charge current density reads

$$J_k = \frac{\sigma_N}{2e} \int_{-\infty}^{\infty} d\varepsilon j_{k3}^0, \quad (7)$$

Here  $\sigma_N = e^2 \nu_F D$  and  $\nu_F$  are the normal-state conductivity and density of states at the Fermi level respectively. In Eq. (5) the term  $H^{ab} = \text{Tr} \tau_b \sigma_a [-i\mathbf{h} \cdot \boldsymbol{\sigma} \tau_3, \hat{g}^K]/8$  describes the Hanle precession of spin caused by the exchange field, and  $R^{ab} = \text{Tr} \tau_b \sigma_a [\check{\Delta}, \hat{g}^K]/8$  the conversion between quasiparticles and the superconducting condensate. Finally  $I_{coll}^{ab} = \text{Tr} \tau_b \sigma_a [\check{\Sigma}, \hat{g}]^K/8$  in Eq. (5) is the collision integral describing the different scattering process with self-energy  $\check{\Sigma}$ . We discuss next different scattering processes.

*Elastic self-energy terms.* We consider elastic contributions to  $\check{\Sigma}_{el}$  due to scattering at impurities with spin-orbit coupling (relaxation time  $\tau_{so}$ ) and the spin flips at magnetic impurities ( $\tau_{sf}$ ) (Maki, 1966). Within the Born approximation, they read  $\check{\Sigma}_{so} = \boldsymbol{\sigma} \cdot \check{g} \boldsymbol{\sigma} / (8\tau_{so})$ ,  $\check{\Sigma}_{sf} = \boldsymbol{\sigma} \cdot \tau_3 \check{g} \tau_3 \boldsymbol{\sigma} / (8\tau_{sf})$ . In the normal state they contribute to the energy-independent total spin-relaxation time  $\tau_{sn}^{-1} = \tau_{so}^{-1} + \tau_{sf}^{-1}$ . In contrast, in the superconducting case the spin-relaxation time and length acquire energy dependence, which is different for the spin-orbit and spin-flip scattering (Maki, 1966; Morten *et al.*, 2004, 2005). Therefore it is convenient to describe the relative strength of these two scattering mechanisms in terms of the parameter  $\beta = (\tau_{so} - \tau_{sf}) / (\tau_{so} + \tau_{sf})$ . In diffusive superconducting thin films one can also describe the depairing effect of an in-plane magnetic field with a self-energy term  $\check{\Sigma}_{orb} = \tau_3 \check{g} \tau_3 / \tau_{orb}$  characterized by the orbital depairing time  $\tau_{orb}$  (Anthore *et al.*, 2003; de Gennes, 1999). This term also contributes to charge imbalance relaxation (Nielsen *et al.*, 1982; Schmid and Schön, 1975).

The parameters  $\tau_{sn}^{-1}$  and  $\beta$  are material specific. For example, in Al films, the reported values from a set of

spin injection experiments are  $\tau_{\text{sn}} \approx 100$  ps (Jedema *et al.*, 2002; Poli *et al.*, 2008) and  $\beta \approx 0.5$  indicating the dominance of spin-flip relaxation over spin-orbit scattering, whereas the reported value of  $\tau_{\text{sn}}$  in Nb is only 0.2 ps, and is strongly dominated by spin-orbit scattering (Wakamura *et al.*, 2014). They affect both the spectrum of a bulk superconductor (see Fig. 3) and the spin relaxation as described in Sec. IV.A.

*Inelastic self-energies.* The relevant inelastic processes entering the self-energy in Eq. (4), are the particle-phonon and particle-particle collisions. These processes do not conserve the energies of colliding quasiparticles, but conserve the total spin.

The coupling between quasiparticles and phonons limits some of the effects discussed in the following sections. Due to the energy dependence of the phonon density of states, this coupling decreases rapidly towards low temperatures, and eventually phonons decouple from electrons, and the main heat relaxation occurs via other processes such as quasiparticle diffusion. Superconductivity modifies the electron-phonon heat conduction (Eliashberg, 1972; Kaplan *et al.*, 1976; Kopnin, 2001), as also the electronic spectrum is energy dependent, and is affected by the spin splitting (Grimaldi and Fulde, 1997; Virtanen *et al.*, 2016).

Particle-particle collisions in superconductors and superfluids are discussed by Eliashberg (1972); Kopnin (2001); and Serene and Rainer (1983), although mainly within contact interaction models disregarding screening effects (Feigel'man *et al.*, 2000; Kamenev and Levchenko, 2009; Narozhny *et al.*, 1999). The collision integrals can have spin structure also in the normal state (Chitchev and Burmistrov, 2008; Dimitrova and Kravtsov, 2008).

The far-from-equilibrium results discussed in Sec. IV disregard the particle-particle collisions, as the simpler theory already describes effects not very far from the measured ones. On the other hand, Sec. V mostly concentrates on the quasiequilibrium limit, where also spin accumulation is lost due to a strong spin relaxation.

*Hybrid interfaces.* In subsequent sections we apply the kinetic equation, Eq. (5), in different situations. For the description of transport in hybrid structures, we need in addition a description of interfaces between different materials in the form of boundary conditions. Such interfaces usually are described by sharp changes of the potential and material parameters over atomic distances, and thus cannot be included directly in the quasiclassical equations which describe properties over distances much larger than  $\lambda_F$ . The description of hybrid interfaces requires then the derivation of suitable boundary conditions, first done in the quasiclassical approach by Zaitsev (1984).

Boundary conditions for the Usadel equation trace back to the work of Kupriyanov and Lukichev (1988). These boundary conditions are applicable for non-

magnetic N-N, S-S and S-N interfaces with low transmissivity (Lambert *et al.*, 1997). Later Nazarov (1999) generalized these boundary conditions for an arbitrary interface transparency.

Tokuyasu *et al.* (1988) derived the boundary condition for an interface between a superconductor and a ferromagnetic insulator and introduced the concept of the spin-mixing angle, which describes the spin-dependent phase shifts acquired by the electrons after being scattered at the FI/S interface. Later Cottet *et al.* (2009) and Zhao *et al.* (2004) extended these boundary conditions to magnetic metallic structures, such as F-S or S-F-S systems, though with low polarization. Boundary conditions for large polarization and low transmission have been presented by Bergeret *et al.* (2012) and Machon *et al.* (2013). General boundary conditions for arbitrary spin polarization and transmission have been extensively discussed by Eschrig *et al.* (2015).

Here we mainly deal with low transmissive barriers between a mesoscopic superconductor and normal and magnetic leads and use the description presented by Bergeret *et al.* (2012). In this description, the component of the spectral current density multiplied by  $\sigma_N$  perpendicular to the interface is continuous across it, and given by

$$\sigma_N j_{\perp,b}^a = -\frac{1}{8eR_{\square}} \text{Tr} \tau_b \sigma_a \left[ \hat{\Gamma} \hat{g}_2 \hat{\Gamma}^{\dagger}, \hat{g} \right]^K, \quad (8)$$

where  $R_{\square}$  is the spin-averaged barrier resistance per unit area, and the spin-dependent transmission is characterized by the tunneling matrix  $\hat{\Gamma} = t\tau_3 + u\sigma_3$ , assuming polarization in the  $z$ -direction. The normalized transparencies satisfy  $t^2 + u^2 = 1$  and are determined from the interface polarization  $|P| \leq 1$  via  $2ut = P$ . The Green's function  $\hat{g}_2$  in the r.h.s of Eq. (8) corresponds to the opposite side of the junction.

### III. NONEQUILIBRIUM MODES IN SPIN-SPLIT SUPERCONDUCTORS

The out-of-equilibrium state in superconducting systems is characterized by the presence of nonequilibrium modes associated with the different electronic degrees of freedom. For example, injection of an electric current from a normal electrode into a superconductor generates a charge imbalance mode (Clarke, 1972; Hübner *et al.*, 2010; Tinkham, 1972; Tinkham and Clarke, 1972; Yagi, 2006) that diffuses into the S region. This nonequilibrium mode reflects an imbalance of the quasiparticle population between the electron-like and hole-like spectrum branches. The charge imbalance measurements made in the 1970s were to our knowledge the first to study such nonequilibrium modes in non-local multiterminal settings. This technique was later adapted to spintronics, to study the nonequilibrium spin accumulation induced by spin-polarized electrodes (Johnson and Silsbee, 1985).



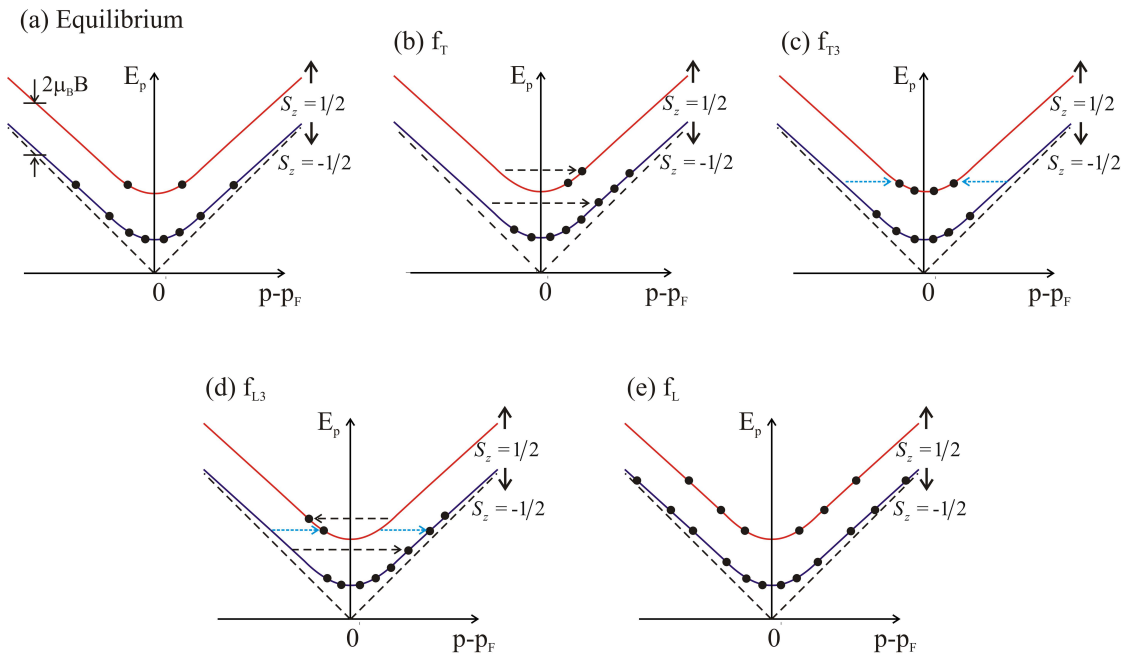


FIG. 4 Schematic illustration of the quasiparticle distribution function components in a superconductor with spin splitting  $2\mu_B B$ . The occupied states are represented by filled circles. (a) Equilibrium distribution, (b) charge imbalance  $f_T$ , (c) spin imbalance  $f_{T3}$ , (d) spin energy imbalance  $f_{L3}$ , and (e) energy imbalance  $f_L$ . The dashed and dotted arrows show elastic processes which lead to the formation — and the reverse processes to the relaxation — of a particular nonequilibrium mode. In (c,d) the dashed black lines show particle-hole branch transitions while the dotted blue lines correspond to the spin-flip processes.

Schematically, nonequilibrium modes can be represented in terms of the electron/hole branches in the spectrum of the superconductor (Tinkham, 1996), as illustrated in Fig. 4. For example the charge mode can be understood as the imbalance between the electron and hole branches (Fig. 4b). In the absence of spin-dependent fields there is one more nonequilibrium mode: the energy imbalance mode (Fig. 4e). It describes the excess energy stemming from an equal change in the quasiparticle populations of the electron-like and hole-like branches. This energy mode affects charge transport properties indirectly via the self-consistency equation for  $\Delta$ . This mechanism explains, for example, the enhancement of the superconducting transition temperature in the presence of a microwave field (Ivlev *et al.*, 1973; Klapwijk *et al.*, 1977).

In this section we generalize the description in terms of nonequilibrium modes to account for superconductors with spin-split density of states. The spin splitting (energy difference  $2h = 2\mu_B B$  between the black and red dispersion curves in Fig. 4 for spin up/down quasiparticles) gives rise to four distinct quasiparticle branches, electron/hole and spin up/down. These four nonequilibrium modes and their coupling are at the basis of the main effects discussed in this review.

### A. Description of nonequilibrium modes in superconductors with spin splitting

At this point we combine the pictorial description of the nonequilibrium modes (Fig. 4) with the quasiclassical formalism introduced in Sec. II.A and in particular, the Usadel equation. For a description of non-equilibrium properties we need to consider the Keldysh component  $\hat{g}^K$  of the quasiclassical GF [Eq. (2)]. For clarity we first consider a unique spin polarization direction parallel to the  $z$ -axis. From the normalization condition, Eq. (3),  $\hat{g}^K$  can be expressed in terms of the retarded and advanced components and the generalized matrix distribution function  $\hat{f}$  (Langenberg and Larkin, 1986)

$$\hat{g}^K = \hat{g}^R \hat{f} - \hat{f} \hat{g}^A. \quad (9)$$

In the case of only one spin polarization axis, the  $4 \times 4$  matrix distribution function  $\hat{f}$  can be written as the sum of four components<sup>2</sup>

$$\hat{f} = f_L \hat{1} + f_T \tau_3 + (f_{T3} \sigma_3 + f_{L3} \sigma_3 \tau_3). \quad (10)$$

<sup>2</sup> Here we assume a unique spin polarization direction. In the most general case the distribution function has all spin components  $\hat{f} = f_L \hat{1} + f_T \tau_3 + \sum_j (f_{Tj} \sigma_j + f_{Lj} \sigma_j \tau_3)$ .

For historical reasons we use the labeling introduced by Schmid and Schön (1975), generalized for the spin-dependent case. The  $L$ -labeled functions describe longitudinal modes, the (spin) energy degrees of freedom, and are antisymmetric in energy with respect to the Fermi level,  $\varepsilon = 0$ . The  $T$ -labeled functions describe transverse modes and are symmetric in energy. In equilibrium, the distribution function is proportional to the unit matrix in Nambu and spin space, and given by

$$\hat{f}_{eq}(\varepsilon) = (1 - 2n_F)\hat{1} = \tanh(\varepsilon/2T)\hat{1}. \quad (11)$$

We can now turn to the pictorial description of Fig. 4 and associate each component of  $\hat{f}$  in Eq. (10) with a nonequilibrium mode as discussed next.

As shown in Figs. 4(b)–(e), two of these modes have electron-hole branch imbalance,  $f_T$  and  $f_{L3}$ , while  $f_{T3}$  and  $f_L$  are particle-hole symmetric. The filled circles in Fig. 4 represent the occupied states. As a reference, panel (a) corresponds to the equilibrium distribution function  $\hat{f} = f_L^0\hat{1} = \tanh(\varepsilon/2T)\hat{1}$ . In order to excite the nonequilibrium modes,  $f_T$ ,  $f_{T3}$  and  $f_{L3}$ , one only needs to move the populated states (filled circles) between the different spectral branches in an elastic process, i.e., between equal-energy states (marked by horizontal dashed arrows). These modes can also relax back to equilibrium due to elastic scattering processes. The relaxation mechanisms depend on intrinsic material properties, degree and type of disorder, and also on the superconducting spectrum, and are discussed in more detail below.

The last nonequilibrium mode, the deviation of  $f_L$  from  $f_L^0$ , is characterized by a change in the total quasi-particle number and energy content, corresponding to an increase or decrease of the effective temperature. It can be excited by increasing the number of occupied states to higher energies, and its relaxation requires inelastic processes.

In the absence of spin splitting, the charge imbalance is determined by  $f_T$ , and the energy imbalance by  $f_L$ . The spin splitting changes the system properties, mixing the coupling between spin-dependent modes and physical observables [see Eqs. (16) and (17) below]. Qualitatively, the outcome can be seen by counting the number of occupied states on the different branches in Fig. 4. For example, the charge imbalance  $\mu$  is determined by the difference between the number of occupied states in the electron and hole branches. Both  $f_T$  and  $f_{L3}$  components contribute to it, as seen in Figs. 4b and d.

On the other hand, a nonzero spin accumulation  $\mu_z$  can be induced by exciting the modes  $f_{T3}$  or  $f_L$  [Figs. 4(c),(e)]. These two contributions to the total spin accumulation have important differences: The mode  $f_{T3}$  contributes to spin imbalance also in the absence of spin splitting. Spin imbalance in this mode can be induced for example by a spin-polarized injection from a ferromagnetic electrode, in both the normal and the superconducting state. The relaxation of the spin accumulation

created in this way is determined by elastic scattering processes. The second mechanism of inducing spin accumulation is by exciting the longitudinal mode  $f_L$ , in the presence of spin splitting [Fig. 4(e)]. Since energy-conserving transitions do not result in the relaxation of the  $f_L$  mode, this component of the spin imbalance is not suppressed by elastic scattering. In other words, its relaxation can be only provided by inelastic processes, e.g., electron-phonon and electron-electron scattering. This result, obtained here on a phenomenological level, is crucial in understanding the long-range spin signal observed in superconductors, for example by Hübler *et al.* (2012) and discussed in the next sections.

## B. Accumulations in terms of the non-equilibrium modes

Quantitatively, we define the charge and spin accumulations based on the Keldysh component of the GF, Eq. (9),

$$\mu(\mathbf{r}, t) = - \int_{-\infty}^{\infty} \frac{d\varepsilon}{16} \text{Tr} \hat{g}^K(\varepsilon, \mathbf{r}, t) \quad (12)$$

$$\mu_{sa}(\mathbf{r}, t) = \int_{-\infty}^{\infty} \frac{d\varepsilon}{16} \text{Tr} \tau_3 \sigma_a [\hat{g}_{eq}^K(\varepsilon, \mathbf{r}, t) - \hat{g}^K(\varepsilon, \mathbf{r}, t)] \quad (13)$$

whereas the local energy and spin-energy accumulations are given by

$$q(\mathbf{r}, t) = \int_{-\infty}^{\infty} \frac{d\varepsilon}{16} \varepsilon \text{Tr} \tau_3 [\hat{g}_{eq}^K(\varepsilon, \mathbf{r}, t) - \hat{g}^K(\varepsilon, \mathbf{r}, t)] \quad (14)$$

$$q_{sa}(\mathbf{r}, t) = \int_{-\infty}^{\infty} \frac{d\varepsilon}{16} \varepsilon \text{Tr} \sigma_a [\hat{g}_{eq}^K(\varepsilon, \mathbf{r}, t) - \hat{g}^K(\varepsilon, \mathbf{r}, t)]. \quad (15)$$

Above,  $a = 1, 2, 3$  denotes the polarization direction of the nonequilibrium spins and energy is counted with respect to the potential  $\mu_S$  of the superconducting condensate (see below).

In terms of the distribution functions, the charge and spin accumulations read (we assume magnetization in  $z$ -direction)

$$\mu = -\frac{1}{2} \int_{-\infty}^{\infty} d\varepsilon (N_+ f_T + N_- f_{L3}) \quad (16)$$

$$\mu_z = -\frac{1}{2} \int_{-\infty}^{\infty} d\varepsilon [N_+ f_{T3} + N_- (f_L - f_{eq})], \quad (17)$$

where  $N_+ = N_\uparrow + N_\downarrow$  is the total density of states (DOS),  $N_- = N_\uparrow - N_\downarrow$  is the DOS difference between the spin subbands, and  $f_{eq}(\varepsilon) = \tanh(\varepsilon/2T)$  is the equilibrium distribution function. Similarly for (14,15) we get

$$q = \frac{1}{2} \int_{-\infty}^{\infty} d\varepsilon \varepsilon [N_+ (f_L - f_{eq}) + N_- f_{T3}] \quad (18)$$

$$q_{sa} = \frac{1}{2} \int_{-\infty}^{\infty} d\varepsilon \varepsilon [N_- (f_L - f_{eq}) + N_+ f_{T3}]. \quad (19)$$

All these quantities, Eqs. (12-15) are directly related to experimental observables. The charge imbalance  $\mu$  characterizes the potential of the quasiparticles in the superconductor (Artemenko and Volkov, 1979). In nonequilibrium situations,  $\mu$  can differ from the condensate potential  $\mu_S$ . In the problems discussed in this Colloquium,  $\Delta$  can be chosen time-independent and  $\mu_S = 0$ . The charge density depends on  $\mu$  via  $\rho = -\nu_F e^2 \phi - e\nu_F \mu$  where  $\phi$  is the electrostatic scalar potential (Kopnin, 2001). In metals, local charge neutrality is maintained on length scales large compared to the Thomas-Fermi screening length, so that  $-e\phi = \mu$  and charge imbalance is associated with static electric fields.

In the quasiclassical formulation used here, electrochemical potential differences appear explicitly in energy shifts in the boundary conditions for the distribution functions (Belzig *et al.*, 1999). The Fermi distribution at potential  $V$  corresponds to

$$f_{\text{eq},L(T)}(E) = \frac{1}{2} \left[ \tanh\left(\frac{E + eV}{2T}\right) + (-) \tanh\left(\frac{E - eV}{2T}\right) \right]. \quad (20)$$

For superconductor at equilibrium,  $V = 0$  in this description. However,  $V = \phi \neq 0$  can describe voltage-biased normal ( $\Delta = 0$ ) reservoirs.

Spin accumulation is a standard observable in spintronics (Jedema *et al.*, 2002; Johnson and Silsbee, 1985). The local energy accumulation is typically measured via electron thermometry (Giazotto *et al.*, 2006). The spin-energy accumulation was measured recently in normal-state nanopillar spin valves (Dejene *et al.*, 2013). To our knowledge this quantity has not been directly studied experimentally in superconducting systems.

In the normal state the spectrum is trivial,  $g^{R(A)} = \pm\tau_3\sigma_0$ . Thus, according to Eq. (9), the Keldysh component is simply proportional to the distribution function. In other words, the different modes decouple in Eqs. (12-15). Moreover, in the normal state it is unnecessary to separate between transverse and longitudinal modes, and rather consider the spin-dependent full distribution function  $f_j(E) = [1 - f_{Lj}(E) - f_{Tj}(E)]/2$ . Solutions of the kinetic equation in the normal state are discussed for example by Brataas *et al.* (2006).

In the superconducting case the situation is more complex. First, the spectrum is strongly energy dependent around the Fermi level and the spectral GFs have a non-trivial structure in spin space. Components proportional to the unit matrix in spin space describes the BCS singlet GFs, whereas terms proportional to the Pauli matrices  $\sigma_j$ ,  $j = 1, 2, 3$ , describe the triplet state (Bergeret *et al.*, 2001b, 2005). Second, due to this energy dependence and non-trivial spin structure, the spectral functions enter (12-15) and lead to a coupling between the different non-equilibrium modes that in turns couple all electronic degrees of freedom, as discussed next.

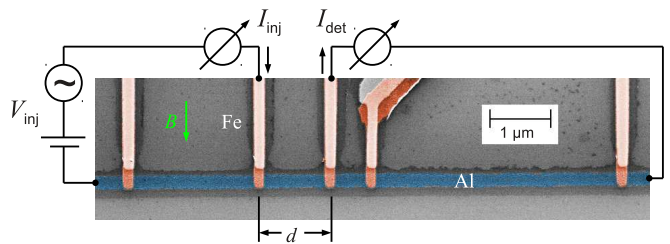


FIG. 5 Scanning electron microscopy image of the lateral structure used by Hübler *et al.* (2012). From Hübler *et al.* (2012).

#### IV. SPIN INJECTION AND DIFFUSION IN SUPERCONDUCTORS

Non-equilibrium modes can be experimentally studied by means of non-local transport measurements. In this section we review experiments on charge and spin injection in superconductors, and apply the kinetic equation approach described in the previous sections to describe different experimental situations.

##### A. Detection of spin and charge imbalance: Non-local transport measurements

Studies of the nonequilibrium modes started with the pioneering experiment of Clarke (1972), who realized a way of detecting the charge imbalance in a superconductor. The main idea of this experiment is to inject a current from a normal metal (injector) into a superconductor. This current creates a charge imbalance that corresponds to a shift of the chemical potential of the quasiparticles with respect to the one of the condensate. This shift of the chemical potential can be detected by a second electrode (detector) that probes the voltage between the superconductor and the detector.

More recent experiments used the same non-local measurement to explore the charge, energy and spin modes in mesoscopic superconducting lateral structures (Beckmann *et al.*, 2004; Hübler *et al.*, 2010; Poli *et al.*, 2008; Quay *et al.*, 2013; Wolf *et al.*, 2014a, 2013). A scanning electron microscopy image of such a lateral structure is shown in Fig. 5. A detailed overview of the experiments on charge and energy imbalance can be found in the recent topical reviews by Beckmann (2016) and Quay and April (2017).

Whereas the charge and energy modes were known for a long time, it was first in the 1990s that theorists predicted that electronic charge and spin degrees of freedom can be separated in a superconductor (Kivelson and Rokhsar, 1990; Zhao and Hershfield, 1995). First experiments on F-S-F layered structures, however, did not show any evidence of such a spin-charge separation (Gu *et al.*, 2002; Johnson, 1994) and the different relaxation times for spin and charge accumulation in superconductors re-

mained an open question.

First clear insight into the separation of the spin and charge modes was obtained in experiments using lateral nanostructures with ferromagnetic injectors and detectors (Beckmann *et al.*, 2004; Cadden-Zimansky *et al.*, 2007; Hübler *et al.*, 2012; Kolenda *et al.*, 2016; Poli *et al.*, 2008; Quay *et al.*, 2013; Shin *et al.*, 2005; Wolf *et al.*, 2013, 2014b; Yang *et al.*, 2010). First theoretical works on spin injection into mesoscopic superconductors (Morten *et al.*, 2004, 2005) showed that the spin-relaxation length in the superconducting state strongly depends on the energy of the injected quasiparticles and on the spin relaxation mechanism. In particular, for a dominating spin-orbit scattering, superconductivity suppresses the spin relaxation rate  $\tau_s^{-1}$ , which can be qualitatively understood as the decrease in the cross section of the quasiparticle momentum scattering at the energies near the gap edge  $\varepsilon \sim \Delta$ . The suppression of  $\tau_s^{-1}$  is however compensated by the decrease in the quasiparticle group velocity  $v_g \sim v_F \sqrt{1 - |\Delta|^2/\varepsilon^2}$  so that the spin relaxation length  $\lambda_{so} \sim v_g \tau_s$  remains almost unchanged in the superconducting state. On the contrary, if the spin-flip mechanism dominates, the spin relaxation is not related to the momentum scattering because the interaction with magnetic impurities does not depend on the propagation direction and the quasiparticle spin does not depend on energy. This results in an increase of  $\tau_s^{-1}$  which is equivalent to a decrease of the spin-relaxation length in the superconducting state. Although these works provided an explanation to some experiments, two important features observed in subsequent works could not be explained in terms of that theory: First, the spin accumulation was detected at distances from the injector much larger than the spin-relaxation length measured in the normal state (Hübler *et al.*, 2012; Quay *et al.*, 2013; Wolf *et al.*, 2013). Second, an unexpected spin accumulation was observed even if the current was injected from a non-magnetic electrode (Wolf *et al.*, 2013). In order to explain these two observations one needs to take into account the spin splitting in the superconductor.

### B. Non-local conductance measurements in spin-split superconductors

Specifically, one of the setups studied by Hübler *et al.* (2012), was a lateral non-local spin valve (see Fig. 5) where the experimentalists determined the non-local differential conductance

$$g_{nl} = \frac{dI_{\text{det}}}{dV_{\text{inj}}}. \quad (21)$$

Typical experimental curves are shown in Fig. 6a, adapted from Hübler *et al.* (2012) and Fig. 6b shows the results calculated from the kinetic equations.

If the detector is a ferromagnet with magnetization collinear with the spin accumulation in the wire, the

current at the detector for  $V_{\text{det}} = 0$  is obtained from Eqs. (7,8),

$$I_{\text{det}} = (\mu + P_{\text{det}}\mu_z)/R_{\text{det}}, \quad (22)$$

where  $R_{\text{det}} = R_{\square}/A$  is the detector interface resistance in the normal state,  $A$  is the cross-sectional area of the detector,  $\mu$  is the charge imbalance and  $\mu_z$  the spin imbalance defined in Eqs. (12,13). According to the explicit expressions (16,17), the full description of the non-local current requires all four non-equilibrium modes.

Particularly interesting is the contribution from the second term in the r.h.s. of Eq. (17). It is nonzero when the spin splitting described by  $N_-$  is nonzero and it provides a qualitative explanation of the experiments by Hübler *et al.* (2012); Quay *et al.* (2013); and Wolf *et al.* (2013): The spin imbalance  $\mu_z$ , being related to the energy nonequilibrium mode  $f_L$ , once excited can only relax via inelastic processes, especially mediated by the electron-phonon interaction. At low temperatures the corresponding decay length can be much larger than the spin decay length in normal metals. This explains the long-range non-local signal observed in the experiments. The observed long-range spin accumulation can thus be understood to result from the spin accumulation generated by the effective heating of the superconducting wire caused by the injection of nonequilibrium quasiparticles with energies larger than the superconducting gap (Bobkova and Bobkov, 2015, 2016; Krishtop *et al.*, 2015; Silaev *et al.*, 2015a,b; Virtanen *et al.*, 2016). Such a heating can originate, for example, by an injected current even from the non-ferromagnetic electrode. The heating is not sensitive to the sign of the bias voltage at the injector and hence the generated spin imbalance must be an even function of the voltage,  $\mu_z(V_{\text{inj}}) = \mu_z(-V_{\text{inj}})$ . This leads to an antisymmetric shape of the non-local spin signal in  $g_{nl}$  with respect to  $V_{\text{inj}}$ , in agreement with the experimental observation (Wolf *et al.*, 2014a). All these features occur only if the superconductor has a spin-split density of states induced either by an external magnetic field or by the proximity to a ferromagnetic insulator.

A quantitative description of these effects can be provided by solving the kinetic equations for superconductors with spin-split subbands (Silaev *et al.*, 2015a). In this case the diffusion couples non-equilibrium modes pairwise. In particular, the kinetic equations (5) take the form

$$\nabla \cdot \begin{pmatrix} j_e \\ j_s \\ j_c \\ j_{se} \end{pmatrix} = \begin{pmatrix} 0 & 0 & 0 & 0 \\ 0 & 0 & 0 & S_{T3} \\ 0 & 0 & R_T & R_{L3} \\ 0 & 0 & R_{L3} & R_T + S_{L3} \end{pmatrix} \begin{pmatrix} f_L \\ f_{T3} \\ f_T \\ f_{L3} \end{pmatrix}, \quad (23)$$

where the spectral energy  $j_e$ , spin  $j_s$ , charge  $j_c$  and spin

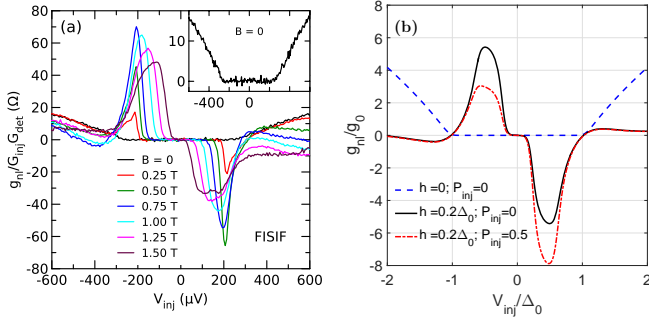


FIG. 6 (a) Nonlocal conductance measured as a function of the injecting voltage,  $g_{nl}(V_{inj})$  adopted from Hübler *et al.* (2012). (b) The same quantity calculated using the kinetic theory for  $\alpha_{orb} = 1.33$ ,  $\beta = 0.5$ ,  $(\tau_{sn}T_{c0})^{-1} = 0.2$ ,  $T = 0.05T_{c0}$ , effective inelastic relaxation length  $L = 20\lambda_{sn}$ ,  $L_{det} = 5\lambda_{sn}$ . Black solid and red dash-dotted curves correspond to the injection from non-ferromagnetic ( $P_{inj} = 0$ ) and ferromagnetic ( $P_{inj} = 0.5$ ) electrodes, respectively at the spin-splitting  $h = 0.2\Delta_0$ . Blue dashed line corresponds to  $h = 0$ . The conductance is normalized to  $g_0 = R_\xi/(R_{inj}R_{det})$ , where  $R_\xi = \xi/(A_s\sigma_N)$  is the normal-state resistance of the wire with length  $\xi$  and cross section  $A_s$ .

energy  $j_{se}$  currents derived from the general Eq.(6) are

$$\begin{pmatrix} j_e \\ j_s \\ j_c \\ j_{se} \end{pmatrix} = \begin{pmatrix} D_L & D_{T3} & 0 & 0 \\ D_{T3} & D_L & 0 & 0 \\ 0 & 0 & D_T & D_{L3} \\ 0 & 0 & D_{L3} & D_T \end{pmatrix} \begin{pmatrix} \nabla f_L \\ \nabla f_{T3} \\ \nabla f_T \\ \nabla f_{L3} \end{pmatrix}. \quad (24)$$

Here  $D_{L/T/T3/L3}$  are kinetic coefficients related to the spectral GFs (Silaev *et al.*, 2015a),  $S_{T3/L3}$  are parts of collision integrals describing spin relaxation, and  $R_{T/L3}$  the coupling between the quasiparticles and the superconducting condensate.

On the one hand, the charge is coupled to the spin-energy mode [lower right block of Eq. (24)]. The relaxation of both of these modes, right hand side of Eq. (23), is nonvanishing for all energies, below and above the gap due to the magnetic pair breaking effects (Nielsen *et al.*, 1982; Schmid and Schön, 1975). On the other hand, the spin-splitting field couples the spin and energy modes,  $f_L$  and  $f_{T3}$  respectively [upper left block of Eq. (24)]. As explained above, the energy mode can only decay via inelastic scattering which at low temperature can be disregarded compared to the spin relaxation.

Solutions of Eqs. (23,24) along with Eqs. (16,22) reproduce the main features of the measured non-local conductance presented in Fig. 6a. Depending on the magnitudes of the spin-splitting field  $h$  and the injector polarization  $P_{inj}$ , we can identify three distinct parameter regimes affecting the symmetry of  $g_{nl}$ . (i) When  $h = P_{inj} = 0$  (blue dashed curve in Fig. 6b), the only contribution to the detector current comes from charge imbalance and  $g_{nl}$  is a symmetric function of the injection voltage. In the absence of spin splitting and depairing effects,  $R_T = 0$  for

$\varepsilon > \Delta$ , and hence charge imbalance decays only via inelastic scattering neglected here. This explains the monotonic increase of  $g_{nl}$  in Fig. 6b at large voltages. (ii) For  $P_{inj} = 0$  but in the presence of an applied field leading to  $h \neq 0$  (black solid curve), charge relaxation is strongly enhanced due to the orbital depairing. The main long-range contribution comes from  $\mu_z$  produced by the heating effect described above. The resulting  $g_{nl}$  is an anti-symmetric function of  $V_{inj}$ . (iii) When both  $h \neq 0$  and  $P_{inj} \neq 0$  (red dash-dotted curve), an additional symmetric long-range contribution in  $g_{nl}$  results due to a thermoelectric effect at the injector. Note that in the case  $h = 0$ ,  $P_{inj} \neq 0$ , there would be another symmetric contribution to  $g_{nl}$  due to the regular spin injection also present in the normal state. However, this is a short-range mode (decays via spin relaxation), and therefore does not show up beyond the spin relaxation length.

In the experiments by Hübler *et al.* (2012); Quay *et al.* (2013); and Wolf *et al.* (2014a) the spin-splitting field was caused by an external magnetic field. Therefore one needs to take into account the orbital depairing effect of the magnetic field in addition to the Zeeman effect. The relative strength of the orbital depairing and the spin-splitting field is described by the dimensionless parameter  $\alpha_{orb} = (h\tau_{orb})^{-1}$ . In Fig. 6 we choose the value  $\alpha_{orb} = 1.33$ , which should correspond to the experiment by Hübler *et al.* (2012).

In the presence of a supercurrent, all coefficients of the matrix in Eq. (24) are nonzero (Aikebaier *et al.*, 2017). As a result, for example the spin and charge modes are directly coupled by diffusion.

### C. Spin Hanle effect

In the previous sections we assume that all magnetizations and the applied field are collinear. If one lifts this assumption, the applied field leads to a precession of the injected spin around the field direction. This is the spin Hanle effect that in the normal state has been extensively studied in the literature and observed in several experiments (Jedema *et al.*, 2001, 2003; Johnson and Silsbee, 1985; Villamor *et al.*, 2015; Yang *et al.*, 2008). The Hanle precession can be measured via the non-local conductance in a setup such as the one shown in Fig. 5. The non-local measured signal oscillates and decays as a function of the amplitude of the applied field.

Formally the Hanle effect is described by the first term on the r.h.s of Eq. (5). Indeed, one can derive the Bloch-Torrey transport equation (Torrey, 1956) for the magnetic moment  $\mathbf{m}(\varepsilon, x) = \text{Tr}(\tau_3 \sigma g^K)/8$  from Eq. (5) (Silaev *et al.*, 2015b). It reads

$$\frac{\partial \mathbf{m}}{\partial t} + \nabla \cdot \mathbf{j}_s = \gamma \mathbf{m} \times \mathbf{h}_s - \mathbf{m}/\tau_S. \quad (25)$$

Here  $\gamma = -2$  is the electron gyromagnetic ratio and  $\mathbf{j}_s$  is the spin current density tensor. In the normal state

the spin relaxation  $\tau_S$  and Zeeman field  $\mathbf{h}_s$  are energy independent. This explains why the nonlocal resistance vs. field curve does not depend either on temperature or on the type of spin relaxation (magnetic or spin-orbit impurities). In contrast, they are predicted to be strongly energy dependent in the superconducting state, and the precession and decay of the nonlocal signal disappear at  $T \rightarrow 0$ , whereas the shape of the curves at intermediate temperatures depends on the type of spin relaxation (Silaev *et al.*, 2015b). Experimental evidence of the Hanle effect in the superconducting state has not been reported so far.

#### D. Spin imbalance by ac excitation

The quasiparticle  $f_{T,j}$  mode — or equivalently, the quasiparticle magnetic moment  $\mathbf{m}(\varepsilon, x)$  above — can be excited by an external ac magnetic field, which via the Zeeman coupling generates a conduction electron spin resonance (Aoi and Swihart, 1970; Maki, 1973; Nemes *et al.*, 2000; Vier and Schultz, 1983; Yafet *et al.*, 1984). This was recently studied experimentally in spin-split thin Al films by Quay *et al.* (2015). As the  $f_{T,j}$  mode can relax rapidly via elastic spin-flip scattering, the linewidth seen in such experiments is generally  $\tau_S^{-1} \simeq \tau_{sn}^{-1}$  instead of the time scale of the long-ranged non-local spin signal. Spin-flip scattering also provides a channel via which electromagnetic fields can generate spin imbalance through the orbital coupling (van Bentum and Wyder, 1986; Virtanen *et al.*, 2016). For high enough driving amplitude, the imbalance modifies the self-consistent  $\Delta(T)$  relation, which develops additional features in the spin-split case (Eliashberg, 1970; Virtanen *et al.*, 2016). Effects related to spin-splitting and relaxation can moreover be probed with tunnel junctions at low frequencies (Quay *et al.*, 2016) or via photoassisted tunneling (Marchegiani *et al.*, 2016).

#### V. THERMOELECTRIC EFFECTS

Thermoelectric effects relate temperature differences to charge currents, and electrical potentials to heat currents. Thermoelectric effects are typically described via the linear response relation between charge and heat currents  $I$ ,  $\dot{Q}$  and bias voltage and temperature difference

$V$  and  $\Delta T$  across a contact:<sup>3</sup>

$$\begin{pmatrix} I \\ \dot{Q} \end{pmatrix} = \begin{pmatrix} G & \alpha \\ \alpha & G_{\text{th}}T \end{pmatrix} \begin{pmatrix} V \\ -\Delta T/T \end{pmatrix}. \quad (26)$$

Here  $G$  is the conductance and  $G_{\text{th}}$  the heat conductance of the contact.  $\alpha$  is the thermoelectric coefficient.

With a non-zero  $\alpha$ , electrical energy may be converted to heat or cooling, or reciprocally a temperature difference may be converted to electrical power. The efficiency of this conversion is typically described by the thermoelectric figure of merit,

$$ZT = \frac{\alpha^2}{G_{\text{th}}GT - \alpha^2} = \frac{S^2GT}{\tilde{G}_{\text{th}}}, \quad (27)$$

where  $S = \alpha/(GT)$  is the thermopower (Seebeck coefficient) and  $\tilde{G}_{\text{th}} = G_{\text{th}} - \alpha^2/(GT)$  is the thermal conductance at a vanishing current. In particular, the maximum efficiency of a thermoelectric heat engine is (Snyder and Ursell, 2003)  $\max \eta = \eta_{\text{Carnot}} \frac{\sqrt{1+ZT}-1}{\sqrt{1+ZT}+1}$  with  $\eta_{\text{Carnot}} = \Delta T/T$ . Maximum efficiencies of the device are obtained when  $ZT \rightarrow \infty$ . At or above room temperature, the record-high figures of merit are obtained in certain strongly doped semiconductor structures (Kim *et al.*, 2015; Zhao *et al.*, 2016). A typical record value for those cases is  $ZT \gtrsim 1 \dots 2$ .

The traditional view of thermoelectric effects in superconductors is that if they exist, they must be very weak. In bulk superconductors, this is partially because any thermoelectrically generated quasiparticle current is easily screened by a supercurrent (Meissner, 1927).

Alternatively, one could then measure this supercurrent via an additional constraint to the phase of the superconducting order parameter in bimetallic multiply connected structures (Ginzburg, 1944). However, even this thermally created phase gradient tends to be weak, owing to the near-complete electron-hole symmetry in superconductors. Galperin *et al.* (1974) showed that

$$\alpha = \alpha_N G(\Delta/T), \quad G(x) = \frac{3}{2\pi^2} \int_x^\infty \frac{y^2 dy}{\cosh^2(y/2)}, \quad (28)$$

where the latter form comes from the reduction of the quasiparticle density in the superconducting state, and  $\alpha_N$  is the value of the thermoelectric coefficient in the

<sup>3</sup> In the case of thermoelectric effects, it is customary to talk about heat currents  $\dot{Q}$  instead of energy currents  $\dot{U}$ , and we adapt this convention here. These are related by (Ashcroft and Mermin, 1976)  $\dot{Q} = \dot{U} - \mu I/e$ , where  $\mu$  is a reference energy compared to the Fermi level. At linear response we can set  $\mu = 0$  in which case  $\dot{Q} = \dot{U}$ . On the other hand, when considering heat balance at non-vanishing voltages as in Sec. V.A, the two are not the same and rather the heat current  $\dot{Q}$  should be used.

normal state. The precise value of  $\alpha_N$  depends on the exact electronic spectrum. For example, for a simple quadratic dispersion  $\alpha_N = \frac{\pi^2 G_T k_B^2 T}{6eE_F}$ , where  $E_F$  is the Fermi energy. At temperatures  $T \ll \Delta/k_B$ ,  $\alpha$  is thus expected to be a product of two small coefficients,  $\alpha_N \propto k_B T/E_F$ , and  $G(\Delta/T)$ . This is very small and not easy to measure quantitatively.

However, superconductors do contain some ingredients for strong thermoelectric effects, because the latter typically require strongly energy dependent density of states of the charge carriers. This is provided by the BCS density of states. Hence, if one can break the electron-hole symmetry of the transport process via some mechanism, superconductors can become very strong thermoelectrics. This is precisely what happens in spin-split superconductors, as an exchange field breaks the symmetry in each spin sector, but so that the overall spin-summed energy spectrum remains electron-hole symmetric. Transport through a spin filter to a spin-split superconductor then can provide large thermoelectric effects because the two spins are weighed differently (Machon *et al.*, 2013, 2014; Ozaeta *et al.*, 2014). We discuss these effects in this section.

### A. Charge and heat currents at a spin-polarized interface to a spin-split superconductor

Consider a tunnel contact from a non-superconducting reservoir R to a superconductor S in a spin-splitting field. Let us assume that the tunnel contact is magnetic, so that the conductance through it is spin-polarized. Denoting the spin-dependent conductances in the normal state by  $G_\uparrow, G_\downarrow$  we can parameterize them by the total conductance  $G_T = G_\uparrow + G_\downarrow$  and the spin polarization  $P = (G_\uparrow - G_\downarrow)/G_T$ . The total tunneling quasiparticle charge and heat currents are now expressed as a sum over spin-dependent contributions, but otherwise of the standard form (Giaever and Megerle, 1961; Giazotto *et al.*, 2006). Denoting the spin-dependent reduced density of states via  $N_+ = N_\uparrow + N_\downarrow$  and  $N_- = N_\uparrow - N_\downarrow$  the spin-averaged tunnel currents can be obtained from the Keldysh component of Eq. (8) after taking the corresponding traces:

$$I = \frac{G_T}{2e} \int_{-\infty}^{\infty} d\varepsilon (N_+ + PN_-) (f_R - f_S) \quad (29)$$

$$\dot{Q}_i = \frac{G_T}{2e} \int_{-\infty}^{\infty} d\varepsilon (\varepsilon - \mu_i) (N_+ + PN_-) (f_R - f_S). \quad (30)$$

Here  $f_{R/S} = n_F(E - \mu_{R/S}; T_{R/S})$ ,  $n_F(E; T) = \{\exp[E/(k_B T)] + 1\}^{-1}$  are the (Fermi) functions of the reservoirs biased at potentials  $\mu_{R/S}$  and temperatures  $T_{R/S}$ . The reduced density of states in the superconductor for spin  $\sigma$  is  $N_\sigma(\varepsilon)$ . The heat current  $\dot{Q}_\sigma^i$  is calculated separately for  $i = R, S$ , using the potential  $\mu_{R/S}$ ,

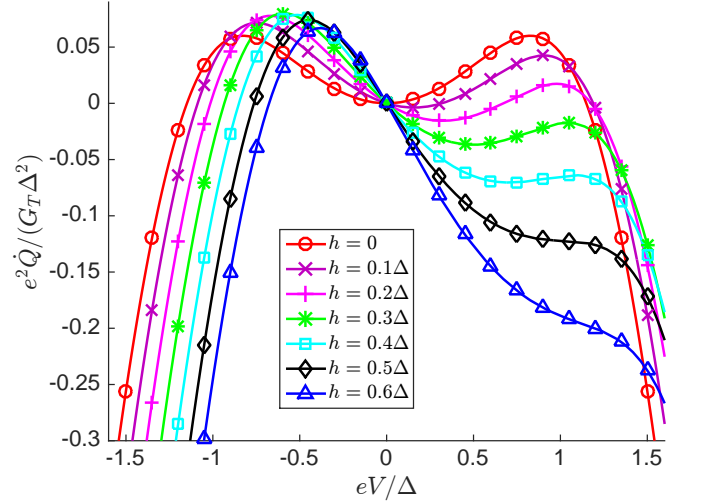


FIG. 7 Cooling power from reservoir R vs. voltage for different values of the exchange field  $h$ , assuming a unit polarization  $P = 1$  at the temperature  $k_B T = 0.3\Delta$  close to that yielding optimal cooling for  $P = h = 0$ . The exchange fields are given in units of  $\Delta$ . Changing the sign of  $P$  or  $h$  inverts the voltage dependence with respect to  $V = 0$ .

because the two heat currents differ by the Joule power  $I(\mu_R - \mu_S)/e$ . In the analysis below, we disregard the spin relaxation effects on the density of states, because this assumption allows for some analytically treatable limits and because it is a fair approximation in the case of often used Al samples.

The heat current from R is a non-monotonous function of voltage even in the absence of spin polarization or temperature difference. In particular, for voltage  $V = (\mu_R - \mu_S) \approx \Delta/e$ , it is positive, i.e., reservoir R cools down (Leivo *et al.*, 1996; Nahum *et al.*, 1994; Pekola *et al.*, 2004). This heat current is quadratic in the voltage, and therefore it does not result from the usual Peltier effect [Eq. (26) for  $\dot{Q}$ ] where the cooling power is linear in voltage.

Interestingly, in the presence of spin polarization  $P$  and with a non-zero spin-splitting field  $h$  in the superconductor, the cooling power is nonzero even in the linear response regime, *i.e.* low voltages (Ozaeta *et al.*, 2014). As an example we show in Fig. 7 the cooling power from reservoir R as a function of voltage for various values of  $h$ , assuming the ideal case of unit spin polarization  $P = 1$ .

Contrary to the spin-independent case, the N-FI-S element can also be used to refrigerate the superconductor. Electron refrigeration using magnetic elements have been studied by Rouco *et al.* (2018).

### B. Linear response: heat engine based on a superconductor/ferromagnet structure

As can be seen in Fig. 7, the simultaneous presence of the non-vanishing spin polarization  $P$  and a spin-splitting

field  $h$  lead to a heat current that has a linear component in the voltage  $V$ . This component is nothing else than the Peltier effect. In the limit  $k_B T \ll \Delta - h$  the linear-response coefficients evaluate to (Ozaeta *et al.*, 2014)

$$G \approx G_T \sqrt{2\pi\tilde{\Delta}} \cosh(\tilde{h}) e^{-\tilde{\Delta}}, \quad (31)$$

$$G_{\text{th}} \approx \frac{k_B G_T \Delta}{e^2} \sqrt{\frac{\pi}{2\tilde{\Delta}}} e^{-\tilde{\Delta}} \left[ e^{\tilde{h}} (\tilde{\Delta} - \tilde{h})^2 + e^{-\tilde{h}} (\tilde{\Delta} + \tilde{h})^2 \right], \quad (32)$$

$$\alpha \approx \frac{G_T P}{e} \sqrt{2\pi\tilde{\Delta}} e^{-\tilde{\Delta}} \left[ \Delta \sinh(\tilde{h}) - h \cosh(\tilde{h}) \right], \quad (33)$$

where  $\tilde{\Delta} = \Delta/(k_B T)$  and  $\tilde{h} = h/(k_B T)$ . These yield the thermopower

$$S = \frac{\alpha}{G_T} \approx \frac{P\Delta}{eT} [\tanh(\tilde{h}) - h/\Delta]. \quad (34)$$

At low temperatures the thermopower is maximized for  $h = k_B T \text{arccosh}[\Delta/(k_B T)]$ , where it is

$$S_{\text{max}} \approx \frac{k_B}{e} P \left[ \frac{\Delta}{k_B T} - \text{arccosh} \left( \sqrt{\frac{\Delta}{k_B T}} \right) \right]. \quad (35)$$

It can hence become much larger than the ‘‘natural scale’’  $k_B/e$ , and even diverge towards low temperatures. However, such a divergence comes together with the vanishing of the conductance, Eq. (31), and therefore is in practice either cut off by circuit effects, where the impedance to the voltmeter becomes lower than the contact impedance, due to spin relaxation neglected above, or alternatively by additional contributions beyond the BCS model. The latter ones are described in more detail by Ozaeta *et al.* (2014). Nevertheless, with proper circuit design one should be able to measure a thermopower much exceeding  $k_B/e$  in this setup.

The above theoretical predictions in the linear response regime were confirmed experimentally by Kolenda *et al.* (2017, 2016). In particular, they prepared a sample containing a crossing of three types of metals, a normal-metallic Cu, ferromagnetic Fe, and superconducting Al. The measured configuration is sketched in Fig. 8a. The electrons in the ferromagnetic wire were heated with the heater current  $I_{\text{heat}}$ , producing a temperature difference between the ferromagnet and the superconductor. The contact between the ferromagnet and the normal metal is ohmic and therefore the temperature difference between them is negligibly small. Then the thermoelectric current was measured as a function of the magnetic field  $\mathbf{B}$  applied parallel to the ferromagnetic wire. The agreement between the experimental results and the above described tunneling theory was excellent (see Fig. 9). The temperature difference between the ferromagnet and the superconductor was a fitting parameter, whereas the polarization  $P$  was fitted from the conductance spectrum. In the experiment it was fitted to the value  $P = 0.08$ , a

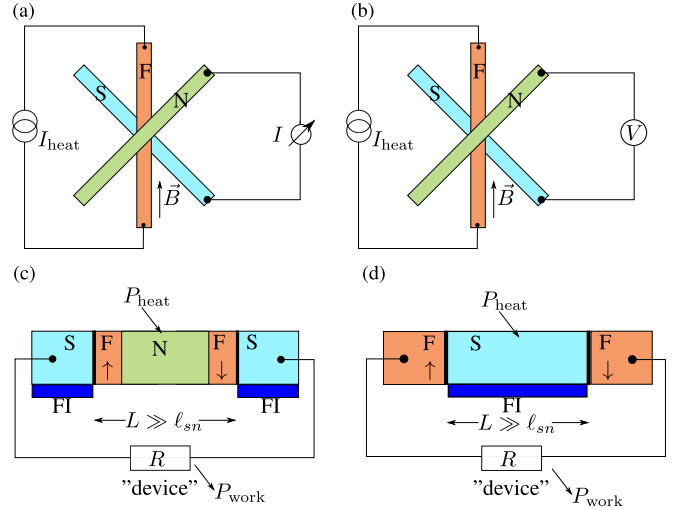


FIG. 8 a) Schematic setup for measuring the thermoelectrically induced current, used by Kolenda *et al.* (2016). S, F, and N stand for a superconductor, ferromagnet and a normal metal, whereas FI is a ferromagnetic insulator. b) Setup used for a direct measurement of the Seebeck effect. c) Heat engine realized in a lateral setup with ‘‘n-doped’’ and ‘‘p-doped’’ junctions using a FNF trilayer with antiparallel magnetization directions. To disregard spin accumulation, the island has to be large compared to the spin relaxation length. d) Heat engine with a spin-split superconducting island. The ferromagnets can also be replaced by a normal metal if the interfaces contain a ferromagnetic insulator. In (c) and (d), the heating power  $P_{\text{heat}}$  is partially converted to ‘‘useful’’ work  $P_{\text{work}}$  dissipated on the load.

modest value attributed to the thin oxide barrier between the Fe and the Al layers. In principle larger values of  $P$  can be obtained by increasing the thickness of the oxide barrier (Münzenberg and Moodera, 2004), but this of course would reduce the amplitude of the thermoelectric current.

In the experiment, the thermoelectric current was measured rather than the voltage. In that case the impedance of the sample dominated that of the measurement lines. This is why the measurement yielded the exponentially low thermoelectric current, which nevertheless was sizeable. The measurement configuration in Fig. 8b would have directly measured the generated voltage drop (*i.e.*, Seebeck effect) instead of the current. This voltage results from the ratio of two exponentially small functions, the thermoelectric coefficient  $\alpha$  and the conductance  $G$ , and itself is not small. Such a measurement would then tell about spurious effects, for example due to spin relaxation, or due to the presence of fluctuations or states inside the gap. These effects would limit the diverging Seebeck coefficient at low temperatures (Ozaeta *et al.*, 2014). Better still, replacing the normal metal with another superconductor with an inverse spin-splitting field, would have resulted to twice as large signal (corresponding to a series of p- and n-doped thermoelectric elements),



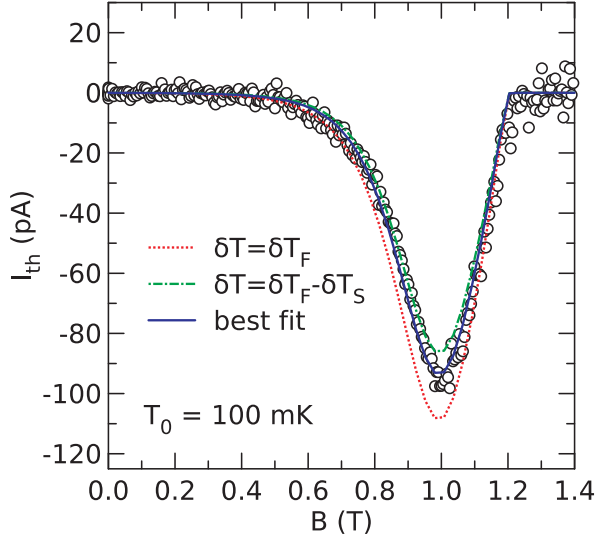


FIG. 9 Thermoelectric current as a function of the applied magnetic field, measured in (Kolenda *et al.*, 2016). The circles show the measurement values, the solid lines show a comparison to Eq. (29). The three solid lines correspond to slightly different temperature differences; for further details, see (Kolenda *et al.*, 2016). From Kolenda *et al.* (2016).

but would not be possible to create as such with a magnetic field. The solution would be furthermore to replace the ferromagnetic wire by an FNF heterostructure [Fig. 8c, where the ferromagnets have antiparallel magnetizations, for example due to different coercive fields, and the normal metal N would serve as a spacer between them]. To reach high figures of merit, the ferromagnetic metals should also be replaced by ferromagnetic insulators, which can reach very high values of spin polarization (see Table I), with  $P$  exceeding 0.9.

The island setup in Figs. 8(c) and (d) also realizes a thermally isolated structure, in contrast to those in (a) and (b). This allows realizing a heat engine, where the voltage measurement is replaced by the “device” to be powered with the engine, with resistance that should be matched to the thermoelectric element. If only the electrons of the ferromagnetic island are heated, the main spurious heat conduction mechanism is due to electron-phonon coupling. In that case it is advantageous to use the structure (d), because the electron-phonon heat conduction is weaker in a superconductor (Heikkilä *et al.*, 2017; Kaplan *et al.*, 1976) than in a normal metal (Wellstood *et al.*, 1994). For example, Fig. 10 shows a prediction for the resulting temperature dependence of the thermoelectric figure of merit  $ZT$  in structure (d), including this spurious heat conduction. In an optimized structure, very large  $ZT$  could thus be expected. In the picture,  $g = 5k_B^5 \sqrt{2\pi} e^2 \Sigma \Omega \Delta^3 / (2G_T)$  is a dimensionless quantity characterizing the relative strength of electron-

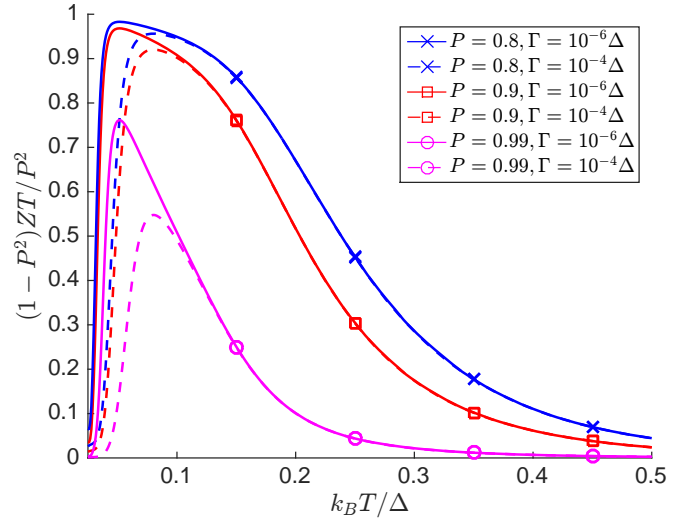


FIG. 10 Figure of merit in a N-FI-S-FI-N heat engine as a function of temperature for polarizations  $P$  of the junction. The figure has been calculated with  $h = 0.5\Delta$  and  $g = 1000$ , without calculating  $\Delta$  self-consistently. The solid lines correspond to  $\Gamma = 10^{-6}\Delta$  and the dashed lines to  $\Gamma = 10^{-4}\Delta$ . The figure of merit at low temperatures reaches very close to  $P^2/(1 - P^2)$  unless  $P$  is very close to unity, but the exact temperature scale where this happens depends on the value of polarization. At the lowest temperatures  $ZT$  is limited by another spurious heat conduction process, due to nonzero density of states inside the gap, described here by the Dynes  $\Gamma$  parameter.

phonon coupling (characterized by  $\Sigma$  (Giazotto *et al.*, 2006)) to the tunnel coupling of the thermoelectric element in an island with volume  $\Omega$ . For example, for  $\Omega = 0.005 \mu\text{m}^3$ ,  $\Sigma = 10^9 \text{ W } \mu\text{m}^{-3}\text{K}^{-5}$  and  $1/G_T = 30 \text{ k}\Omega$ ,  $g = 1000$ .

Note that it is really the presence of the spurious electron-phonon heat conduction that limits the highest available values of  $ZT$ . Often such spurious mechanisms are disregarded from the theoretical analysis, for example in the case of quantum dots (Hwang *et al.*, 2016).

Even if the true figure of merit of the type of heat engine discussed above can be made high, these systems cannot obviously be used to replace room-temperature thermoelectric devices to be applied for example in energy harvesting. However, there are other applications where the large figure of merit may turn out to be essential. For example, this type of thermoelectric heat engine can be used for thermal radiation sensing at low temperatures (Giazotto *et al.*, 2006; Heikkilä *et al.*, 2017). Another possible use of the thermoelectric effects would be in non-invasive low-temperature thermometry (Giazotto *et al.*, 2015b), where the temperature (difference) profiles could be read from the thermopower, without having to apply currents. In a scanning mode this would hence be a low-temperature version of the method used by Menges *et al.* (2016).

Note that the above discussion disregards the effect of spin-orbit or spin-flip scattering on the superconducting state. It limits  $ZT$  especially in heavy-metal superconductors. The associated effects were considered by Bergeret *et al.* (2017) and Rezaei *et al.* (2017).

### C. Spin Seebeck effect

Besides the large thermoelectric effect, the contact between spin-split superconductors with other conducting materials can exhibit a large (longitudinal) spin Seebeck effect, where a temperature difference drives spin currents to/from the spin-split superconductor (Ozaeta *et al.*, 2014). In this case the charge, heat, spin and spin heat currents are described by the full (Jacquod *et al.*, 2012; Machon *et al.*, 2013; Onsager, 1931) Onsager linear-response matrix

$$\begin{pmatrix} I \\ \dot{Q} \\ I_s \\ \dot{Q}_s \end{pmatrix} = \begin{pmatrix} G & \alpha & PG & \tilde{\alpha} \\ \alpha & G_{\text{th}}T & \tilde{\alpha} & PG_{\text{th}}T \\ PG & \tilde{\alpha} & G & \alpha \\ \tilde{\alpha} & PG_{\text{th}}T & \alpha & G_{\text{th}}T \end{pmatrix} \begin{pmatrix} V \\ -\Delta T/T \\ V_s/2 \\ -\Delta T_s/2T \end{pmatrix}, \quad (36)$$

where for  $k_B T \ll \Delta - h$  the coefficients  $G$ ,  $G_{\text{th}}$  and  $\alpha$  are given in Eqs. (31-33), and  $\tilde{\alpha} = \alpha/P$ . Here  $V_s$  and  $\Delta T_s$  refer to spin-dependent biases (Bergeret *et al.*, 2017).

The spin currents induced in the case of two spin-split superconductors, and the additional effects of Josephson coupling, magnetization texture and spin-orbit effects are discussed by Bathen and Linder (2017) and Linder and Bathen (2016). When either of the two materials realizes an island, the spin current can be converted into a spin accumulation  $\mu_z$  that is determined from the balance between thermally induced spin currents and spin relaxation within the island. The above discussion on heat engines assumes a structure size much longer than the spin-relaxation length, and hence disregards this spin accumulation. The effect of the thermally induced spin accumulation on the superconducting gap was considered by Bobkova and Bobkov (2017), who predicted the associated changes in the critical temperature.

This spin Seebeck effect should be contrasted to the analogous phenomenon discussed in non-superconducting materials (Uchida *et al.*, 2014). There, a major contribution to the spin Seebeck signal is due to the thermally induced spin pumping (Hoffman *et al.*, 2013).

### D. Thermophase in a S(FI)S contact

The large thermoelectric effect described above allows for a large thermally induced phase gradient. This was theoretically investigated by Giazotto *et al.* (2015a). The

total current in this case consists of the sum of a thermoelectric current  $I_{\text{th}}$  and the supercurrent,

$$I = I_{\text{th}} + I_c \sin(\varphi), \quad (37)$$

where  $I_{\text{th}}$  is obtained from (29) and  $I_c$  is the critical current for the junction with a phase difference  $\varphi$  of the order parameters across the contact. The critical current is proportional to  $\sqrt{1 - P^2}$  (Bergeret *et al.*, 2012) and depends on the spin-splitting field in S (Bergeret and Giazotto, 2014)

In an electrically open configuration, the two currents must cancel, and instead a *thermophase*  $\varphi^{\text{th}}$  develops across the junction. This is obtained from

$$\sin(\varphi^{\text{th}}) = -\frac{I_{\text{th}}}{I_c}. \quad (38)$$

The thermophase can be detected using a bimetallic loop with two contacts, characterized by critical currents  $I_{c1,2}$  and thermophases  $\varphi_{1,2}^{\text{th}}$ . For non-zero exchange field and spin polarization  $P$ , the resulting thermophases can be much larger than in ordinary bulk superconductors. Hence the temperature dependence of the inductances play a more minor role than in the case of superconductors without spin splitting (Shelly *et al.*, 2016; Van Harlingen *et al.*, 1980). For junctions with non-equal thermophases and for negligible loop inductance (in practice,  $2eLI_{c1,2}/\hbar \ll 1$ ) in the absence of an external flux the circulating current is

$$I_{\text{circ}} = \frac{I_{c1}I_{c2}}{I_{c1} + I_{c2}} [\sin(\varphi_1^{\text{th}}) - \sin(\varphi_2^{\text{th}})]. \quad (39)$$

In the case of symmetric junctions both thermophases are the same and the circulating current in the absence of an external flux vanishes. However, as discussed by Giazotto *et al.* (2015a), the thermoelectric current affects the response of the circulating current to the external flux, allowing for their measurement also in that case.

Equation (38) requires that both sides of the equation have an absolute value of at most unity, i.e.,  $|I_{\text{th}}| < I_c$ . For a very large thermoelectric current, its cancellation with a supercurrent is no longer possible, and instead a voltage across the contact forms. In this case the direct current response of the junction is more similar to the case discussed above in the linear response limit for a N-FI-S junction. This regime was investigated in detail by Linder and Bathen (2016). Moreover, the nonvanishing dc voltage across the superconducting junction leads to Josephson oscillations at the frequency  $2eV/h$ , where  $h$  is the Planck constant. Hence, the device can be used as a temperature (difference) to frequency converter as discussed in more detail by Giazotto *et al.* (2015b).

## VI. SUMMARY AND OUTLOOK

This review focuses on transport and thermal properties of superconducting hybrid structures with a spin-

split density of states. Such a splitting can be achieved either by an external magnetic field, or, more interestingly, by placing a ferromagnetic insulator (FI) adjacent to a superconducting layer (S) (Sec. II). We discuss several experimental situations with the help of a theoretical framework (see Sec. II.A and III.B) based on the quasiclassical formalism, with which one can account for both thermodynamical and nonequilibrium properties of such hybrid structures. In order to account for effects beyond quasiclassics, as for example strong spin polarization, we combine the quasiclassical equations with effective boundary conditions.

Out-of equilibrium superconductivity by itself leads to a decoupling between the charge and energy degrees of freedom of the electronic transport. In this review we show that the combination between superconductivity and magnetism requires on one hand a description of additional nonequilibrium modes, spin and spin energy, and on the other hand to couples them all. This leads to novel and intriguing phenomena discussed in this review with direct impact in latest research activities and proposed future technologies based on superconductors and spin dependent-fields (Eschrig, 2011, 2015; Linder and Robinson, 2015). By using the theoretical formalism presented in this review one can predict and explain phenomena such as the spin injection and relaxation (Sec. IV) in superconductors with an intrinsic exchange field along with their consequences in the transport properties. We also discuss a number of striking thermoelectric effects in superconductors with a spin-splitting field (Sec. V).

The best scenario for the phenomena and applications discussed here, and in particular for the thermoelectric effects, are FI-S systems where the spin splitting can be achieved without the need of an applied magnetic field. Hence it becomes important to look for ideal FI-S material combinations. So far europium chalcogenides (EuO, EuS and EuSe) together with Aluminum films have shown large splittings and hence these are the best combination. In addition, thin films of EuO or EuS can be used as almost perfect spin filters (see Table I) and hence they are good candidates for realizing the near-optimal heat engines proposed in Sec. V. One of the main challenges from this perspective is to find FI-S combinations with large superconducting critical temperature and simultaneously a large spin splitting. Superconductors like Nb or Pb on the one hand increase  $T_C$  with respect to Al-based structures, but on the other the spin-orbit coupling may spoil the sharp splitting as discussed in Sec. II. Recent experiments on GdN-NbN suggest large splittings (Pal and Blamire, 2015) but further research in this direction is needed.

In Sec. IV.D we briefly discuss the dynamics of spin-split superconductors in rf fields. Historically, magnetic resonance effects in superconductors are well studied, but fewer experiments have probed spin-split thin films.

Besides the effects discussed in this review, several the-

oretical studies made striking predictions in mesoscopic systems with spin-split superconductors, such as the creation of highly polarized spin currents (Giazotto and Bergeret, 2013b; Giazotto and Taddei, 2008; Huertas-Hernando *et al.*, 2002), large supercurrents in FI-S-I-S-FI junctions (Bergeret *et al.*, 2001a), junctions with switchable current-phase relations (Strambini *et al.*, 2015), and an almost ideal heat valve based on S-FI elements (Giazotto and Bergeret, 2013a).

Although many of the transport phenomena in spin-split superconductors are now well-understood, we foresee a number of exciting avenues for future research.

One further perspective of the present work is the extension of the Keldysh quasiclassical formalism used in this review to include magneto-electric effects associated with the spin-orbit coupling (SOC). For a linear in momentum SOC the generalization of this can be done by introducing an effective SU(2) gauge potential. The quasiclassical equations in this case have been derived by Bergeret and Tokatly (2013, 2014, 2016). Effects such as the spin-Hall and spin-galvanic effect in superconductors have been studied in the equilibrium case (Konschelle *et al.*, 2015). Extending these results to a nonequilibrium situation, and also to time-dependent fields, would be an interesting further development and would allow for a detailed study of the well-controlled non-linearities associated to these effects in superconductors. First steps in this direction have been taken in (Espedal *et al.*, 2017).

Recent discoveries of skyrmionic states in chiral magnets (Nagaosa and Tokura, 2012) have attracted a lot of attention due to the effects resulting from the interplay of magnetism and SOC (Soumyanarayanan *et al.*, 2016) which can induce chiral Dzyaloshinskii-Moriya interactions between magnetic moments. Currently it is very interesting to study these effects in the presence of the additional component — superconductivity, when the exchange interaction is mediated by the Cooper pairs (de Gennes, 1966b). One can expect that in such systems superconductivity can induce a non-trivial magnetic ordering and dynamics. These effects can show up in various systems including ferromagnet/superconductor bilayers, surface magnetic adatoms and bulk magnetic impurities inducing the localized Yu-Shiba-Rusinov states modified by the SOC (Pershoguba *et al.*, 2015).

Superconducting structures with strong spin-orbit coupling and exchange fields are also of high interest in view of engineering a platform for realization of topological phases and Majorana bound states (Alicea, 2012; Beenakker, 2013; Hasan and Kane, 2010; Qi and Zhang, 2011). Understanding and controlling the behavior and relaxation of nonequilibrium quasiparticles in these systems is also of importance, not least because of their influence on the prospects of solid-state topological quantum computation (Nayak *et al.*, 2008).

This review focuses exclusively on the nonequilibrium properties of superconductors in proximity to magnets.

We expect the inclusion of the magnetization dynamics and its coupling to the electronic degrees of freedom via the reciprocal effects of spin transfer torque and spin pumping (Tserkovnyak *et al.*, 2005) in the far-from equilibrium regime to lead to completely new type of physics, as the two types of order parameters affect each other. The coupling of supercurrent on magnetization dynamics and texture has been studied during the past decade (Houzet, 2008; Richard *et al.*, 2012; Waintal and Brouwer, 2002), but the work where both systems are out of equilibrium has been mainly concentrated on Josephson junctions (Hikino *et al.*, 2011; Holmqvist *et al.*, 2014, 2011; Kulagina and Linder, 2014; Mai *et al.*, 2011) and much less attention has been paid to quasiparticle effects (Linder *et al.*, 2012; Skadsem *et al.*, 2011; Trif and Tserkovnyak, 2013).

Besides the rich physics offered by spin-split superconductors, they have been long used as tools to characterize equilibrium properties of magnets, especially their spin polarization. In this review (see end of Sec. V.B) we outline two further possibilities related to their large thermoelectric response: accurate radiation sensing and non-invasive scanning thermometry. We believe there are also many other avenues to be uncovered, opened by the possibility for realizing a controlled combination of magnetism and superconductivity.

## ACKNOWLEDGMENTS

We thank Faluke Aikebaier, Marco Aprili, Detlef Beckmann, Wolfgang Belzig, Irina Bobkova, Alexander Bobkov, Matthias Eschrig, Yuri Galperin, Francesco Giazotto, Vitaly Golovach, Kalle Kansanen, Alexander Mel'nikov, Jagadeesh Moodera, Risto Ojajärvi, Asier Ozaeta, Charis Quay, Jason Robinson, Mikel Rouco, and Elia Strambini for useful discussions. This work was supported by the Academy of Finland Center of Excellence (Project No. 284594), Research Fellow (Project No. 297439) and Key Funding (Project No. 305256) programs, the European Research Council (Grant No. 240362-Heatronics), the Spanish Ministerio de Economía y Competitividad (MINECO) (Projects No. FIS2014-55987-P and FIS2017-82804-P), the European Research Council under the European Union's Seventh Framework Program (FP7/2007-2013)/ERC Grant agreement No. 615187-COMANCHE.

## REFERENCES

Aasen, David, Michael Hell, Ryan V Mishmash, Andrew Higinbotham, Jeroen Danon, Martin Leijnse, Thomas S Jespersen, Joshua A Folk, Charles M Marcus, Karsten Flensberg, *et al.* (2016), "Milestones toward Majorana-based quantum computing," *Phys. Rev. X* **6** (3), 031016.

Abrikosov, A A, and L. P. Gor'kov (1960a), "Contribution to the theory of superconducting alloys with paramagnetic impurities," *Zh. Eksp. Teor. Fiz.* **39** (6), 1781, [*Sov. Phys. JETP* **12** (6), 1243 (1961)].

Abrikosov, A A, and L. P. Gor'kov (1960b), "On the problem of the Knight shift in superconductors," *Zh. Eksp. Teor. Fiz.* **39** (2), 480, [*Sov. Phys. JETP*, **12** (2), 337 (1961)].

Abrikosov, A A, and L. P. Gor'kov (1962), "Spin-orbit interaction and the Knight shift in superconductors," *Zh. Eksp. Teor. Fiz.* **42** (4), 1088, [*Sov. Phys. JETP*, **15** (4), 752 (1962)].

Aikebaier, Faluke, Mihail A Silaev, and TT Heikkilä (2017), "Supercurrent induced charge-spin conversion in spin-split superconductors," arXiv:1712.08653.

Alicea, J (2012), "New directions in the pursuit of Majorana fermions in solid state systems," *Rep. Progr. Phys.* **75** (7), 076501.

Anthore, A, H. Pothier, and D. Esteve (2003), "Density of states in a superconductor carrying a supercurrent," *Phys. Rev. Lett.* **90**, 127001.

Aoi, K, and J. C. Swihart (1970), "Theory of electron spin resonance in type-I superconductors," *Phys. Rev. B* **2**, 2555–2560.

Artemenko, S N, and A. F. Volkov (1979), "Electric fields and collective oscillations in superconductors," *Sov. Phys. Usp.* **22** (5), 295.

Ashcroft, N W, and N. D. Mermin (1976), *Solid State Physics* (Saunders College, Philadelphia).

Baibich, M N, J. M. Broto, A. Fert, F. Nguyen Van Dau, F. Petroff, P. Etienne, G. Creuzet, A. Friederich, and J. Chazelas (1988), "Giant magnetoresistance of (001)Fe/(001)Cr magnetic superlattices," *Phys. Rev. Lett.* **61**, 2472–2475.

Bardeen, John, Leon N Cooper, and John Robert Schrieffer (1957), "Theory of superconductivity," *Phys. Rev.* **108** (5), 1175.

Bathen, Marianne Etzelmüller, and Jacob Linder (2017), "Spin Seebeck effect and thermoelectric phenomena in superconducting hybrids with magnetic textures or spin-orbit coupling," *Sci. Rep.* **7**, 41409.

Beckmann, D (2016), "Spin manipulation in nanoscale superconductors," *J. Phys.: Condens. Matter* **28** (16), 163001.

Beckmann, D, H. B. Weber, and H. v. Löhneysen (2004), "Evidence for crossed Andreev reflection in superconductor-ferromagnet hybrid structures," *Phys. Rev. Lett.* **93** (19), 197003.

Beenakker, C W J (2013), "Search for Majorana fermions in superconductors," *Annu. Rev. Condens. Matter Phys.* **4** (1), 113–136.

Belzig, Wolfgang, Frank K Wilhelm, Christoph Bruder, Gerd Schön, and Andrei D Zaikin (1999), "Quasiclassical Green's function approach to mesoscopic superconductivity," *Superlatt. Microstruct.* **25** (5), 1251–1288.

van Bentum, P J M, and P. Wyder (1986), "Far-infrared absorption of thin superconducting aluminum films in the pair-breaking and paramagnetic limits," *Phys. Rev. B* **34**, 1582–1594.

Bergeret, F S, K. B. Efetov, and A. I. Larkin (2000), "Nonhomogeneous magnetic order in superconductor-ferromagnet multilayers," *Phys. Rev. B* **62** (17), 11872–11878.

Bergeret, F S, and F. Giazotto (2014), "Manifestation of a spin-splitting field in a thermally biased Josephson junction," *Phys. Rev. B* **89**, 054505.

- Bergeret, F S, and I. V. Tokatly (2013), “Singlet-triplet conversion and the long-range proximity effect in superconductor-ferromagnet structures with generic spin dependent fields,” *Phys. Rev. Lett.* **110** (11), 117003.
- Bergeret, F S, and I. V. Tokatly (2014), “Spin-orbit coupling as a source of long-range triplet proximity effect in superconductor-ferromagnet hybrid structures,” *Phys. Rev. B* **89** (13), 134517.
- Bergeret, F S, and I. V. Tokatly (2016), “Manifestation of extrinsic spin Hall effect in superconducting structures: Nondissipative magnetoelectric effects,” *Phys. Rev. B* **94** (18), 180502.
- Bergeret, F S, A. Verso, and A. F. Volkov (2012), “Electronic transport through ferromagnetic and superconducting junctions with spin-filter tunneling barriers,” *Phys. Rev. B* **86** (21), 214516.
- Bergeret, F S, A. F. Volkov, and K. B. Efetov (2001a), “Enhancement of the Josephson current by an exchange field in superconductor-ferromagnet structures,” *Phys. Rev. Lett.* **86** (14), 3140.
- Bergeret, F S, A. F. Volkov, and K. B. Efetov (2001b), “Long-range proximity effects in superconductor-ferromagnet structures,” *Phys. Rev. Lett.* **86** (18), 4096.
- Bergeret, F S, A. F. Volkov, and K. B. Efetov (2004), “Induced ferromagnetism due to superconductivity in superconductor-ferromagnet structures,” *Phys. Rev. B* **69** (17), 174504.
- Bergeret, F S, Anatoly F Volkov, and Konstantin B Efetov (2005), “Odd triplet superconductivity and related phenomena in superconductor-ferromagnet structures,” *Rev. Mod. Phys.* **77** (4), 1321–1373.
- Bergeret, F Sebastian, Mikhail Silaev, Pauli Virtanen, and Tero T Heikkila (2017), “Nonequilibrium effects in superconductors with a spin-splitting field,” arXiv:1706.08245.
- Binasch, G, P. Grünberg, F. Saurenbach, and W. Zinn (1989), “Enhanced magnetoresistance in layered magnetic structures with antiferromagnetic interlayer exchange,” *Phys. Rev. B* **39**, 4828–4830.
- Bobkova, I V, and A. M. Bobkov (2015), “Long-range spin imbalance in mesoscopic superconductors under Zeeman splitting,” *JETP Lett.* **101** (2), 118.
- Bobkova, I V, and A. M. Bobkov (2016), “Injection of nonequilibrium quasiparticles into Zeeman-split superconductors: a way to create long-range spin imbalance,” *Phys. Rev. B* **93** (2), 024513.
- Bobkova, I V, and A. M. Bobkov (2017), “Thermospin effects in superconducting heterostructures,” *Phys. Rev. B* **96**, 104515.
- Brataas, A, G Bauer, and P Kelly (2006), “Non-collinear magnetoelectronics,” *Phys. Rep.* **427** (4), 157–255.
- Bruno, Ronald C, and Brian B. Schwartz (1973), “Magnetic field splitting of the density of states of thin superconductors,” *Phys. Rev. B* **8**, 3161–3178.
- Buzdin, A I (2005), “Proximity effects in superconductor-ferromagnet heterostructures,” *Rev. Mod. Phys.* **77**, 935–976.
- Buzdin, A I, and L. N. Bulaevskii (1988), “Ferromagnetic film on the surface of a superconductor: Possible onset of inhomogeneous magnetic ordering,” *Sov. Phys. JETP* **67** (3), 576–578.
- Buzdin, AI, L.N. Bulaevskii, and S.V. Panyukov (1982), “Critical-current oscillations as a function of the exchange field and thickness of the ferromagnetic metal ( $f$ ) in an sfs josephson junction,” *JETP Letters* **35**, 178.
- Cadden-Zimansky, P, Z Jiang, and V Chandrasekhar (2007), “Charge imbalance, crossed Andreev reflection and elastic co-tunnelling in ferromagnet/superconductor/normal-metal structures,” *New. J. Phys.* **9** (5), 116.
- Carlson, R V, and A. M. Goldman (1973), “Superconducting order-parameter fluctuations below  $T_c$ ,” *Phys. Rev. Lett.* **31** (14), 880.
- Chandrasekhar, B S (1962), “A note on the maximum critical field of high-field superconductors,” *Appl. Phys. Lett.* **1** (1), 7–8.
- Chtchelkatchev, N, and I Burmistrov (2008), “Energy relaxation in the spin-polarized disordered electron liquid,” *Phys. Rev. Lett.* **100** (20), 206804.
- Clarke, John (1972), “Experimental observation of pair-quasiparticle potential difference in nonequilibrium superconductors,” *Phys. Rev. Lett.* **28**, 1363–1366.
- Clogston, A M (1962), “Upper limit for the critical field in hard superconductors,” *Phys. Rev. Lett.* **9**, 266–267.
- Cottet, Audrey, Daniel Huertas-Hernando, Wolfgang Belzig, and Yu. V. Nazarov (2009), “Spin-dependent boundary conditions for isotropic superconducting Green functions,” *Phys. Rev. B* **80**, 184511.
- Dejene, FK, J. Flipse, G.E.W. Bauer, and B.J. van Wees (2013), “Spin heat accumulation and spin-dependent temperatures in nanopillar spin valves,” *Nat. Phys.* **9**, 636.
- Demler, E A, G. B. Arnold, and M. R. Beasley (1997), “Superconducting proximity effects in magnetic metals,” *Phys. Rev. B* **55** (22), 15174.
- Dimitrova, O V, and V. E. Kravtsov (2008), “Infrared catastrophe in a two-quasiparticle collision integral,” *JETP Lett.* **86** (10), 670–676.
- Dynes, R C, J. P. Garno, G. B. Hertel, and T. P. Orlando (1984), “Tunneling study of superconductivity near the metal-insulator transition,” *Phys. Rev. Lett.* **53**, 2437–2440.
- Eilenberger, Gert (1968), “Transformation of Gorkov’s equation for type II superconductors into transport-like equations,” *Z. Phys.* **214** (2), 195–213.
- Eliashberg, G M (1970), “Film superconductivity stimulated by a high-frequency field,” *JETP Lett.* **11**, 114.
- Eliashberg, G M (1972), “Inelastic electron collisions and nonequilibrium stationary states in superconductors,” *Sov. Phys. JETP* **34**, 668.
- Eltschka, Matthias, Berthold Jäck, Maximilian Assig, Oleg V. Kondrashov, Mikhail A. Skvortsov, Markus Eitzkorn, Christian R. Ast, and Klaus Kern (2014), “Probing absolute spin polarization at the nanoscale,” *Nano Lett.* **14** (12), 7171–7174.
- Eltschka, Matthias, Berthold Jäck, Maximilian Assig, Oleg V. Kondrashov, Mikhail A. Skvortsov, Markus Eitzkorn, Christian R. Ast, and Klaus Kern (2015), “Superconducting scanning tunneling microscopy tips in a magnetic field: Geometry-controlled order of the phase transition,” *Appl. Phys. Lett.* **107** (12), 122601.
- Eschrig, Matthias (2011), “Spin-polarized supercurrents for spintronics,” *Phys. Today* **64** (1), 43.
- Eschrig, Matthias (2015), “Spin-polarized supercurrents for spintronics: a review of current progress,” *Rep. Progr. Phys.* **78** (10), 104501.
- Eschrig, Matthias, Audrey Cottet, Wolfgang Belzig, and Jacob Linder (2015), “General boundary conditions for quasiclassical theory of superconductivity in the diffusive limit: application to strongly spin-polarized systems,” *New. J. Phys.* **17** (8), 083037.

- Espedal, Camilla, Peter Lange, Severin Sadjina, A. G. Mal'shukov, and Arne Brataas (2017), "Spin hall effect and spin swapping in diffusive superconductors," *Phys. Rev. B* **95**, 054509.
- Feigel'man, M V, A. I. Larkin, and M. A. Skvortsov (2000), "Keldysh action for disordered superconductors," *Phys. Rev. B* **61**, 12361–12388.
- Fulde, P, and R. A. Ferrell (1964), "Superconductivity in a strong spin-exchange field," *Phys. Rev.* **135** (3A), A550–A563.
- Galperin, Yu M, V. L. Gurevich, and V. I. Kozub (1974), "Thermoelectric effects in superconductors," *Sov. Phys. JETP* **39** (4), 680.
- de Gennes, P G (1966a), "Coupling between ferromagnets through a superconducting layer," *Phys. Lett.* **23** (1), 10–11.
- de Gennes, P G (1999), *Superconductivity of Metals and Alloys*, Advanced book classics (Perseus, Cambridge, MA).
- de Gennes, PG (1966b), "Coupling between ferromagnets through a superconducting layer," *Phys. Lett.* **23** (1), 10–11.
- Giaever, I, and K. Megerle (1961), "Study of superconductors by electron tunneling," *Phys. Rev.* **122**, 1101–1111.
- Giazotto, F, and F. S. Bergeret (2013a), "Phase-tunable colossal magnetothermal resistance in ferromagnetic Josephson valves," *Appl. Phys. Lett.* **102** (13), 132603–132603–5.
- Giazotto, F, and F. S. Bergeret (2013b), "Quantum interference hybrid spin-current injector," *Appl. Phys. Lett.* **102** (16), 162406.
- Giazotto, F, T. T. Heikkilä, and F. S. Bergeret (2015a), "Very large thermophase in ferromagnetic Josephson junctions," *Phys. Rev. Lett.* **114**, 067001.
- Giazotto, F, P. Solinas, A. Braggio, and F. S. Bergeret (2015b), "Ferromagnetic-insulator-based superconducting junctions as sensitive electron thermometers," *Phys. Rev. Applied* **4**, 044016.
- Giazotto, F, and F. Taddei (2008), "Superconductors as spin sources for spintronics," *Phys. Rev. B* **77**, 132501.
- Giazotto, Francesco, Tero T. Heikkilä, Arttu Luukanen, Alexander M. Savin, and Jukka P. Pekola (2006), "Opportunities for mesoscopies in thermometry and refrigeration: Physics and applications," *Rev. Mod. Phys.* **78**, 217–274.
- Ginzburg, V L (1944), "On the thermoelectric phenomena in superconductors," *Zh. Eksp. Teor. Fiz.* **14**, 134.
- Ginzburg, V L (1957), "Ferromagnetic superconductors," *Sov. Phys. JETP* **4**, 153.
- Grimaldi, Claudio, and Peter Fulde (1997), "Nonequilibrium superconductivity in spin-polarized superconducting tunneling junctions," *Phys. Rev. B* **56**, 2751–2763.
- Gu, J Y, J. A. Caballero, R. D. Slater, R. Loloee, and W. P. Pratt Jr (2002), "Direct measurement of quasiparticle evanescent waves in a dirty superconductor," *Phys. Rev. B* **66** (14), 140507.
- Hao, X, J. S. Moodera, and R. Meservey (1990), "Spin-filter effect of ferromagnetic europium sulfide tunnel barriers," *Phys. Rev. B* **42**, 8235–8243.
- Hasan, M Z, and C. L. Kane (2010), "Colloquium: Topological insulators," *Rev. Mod. Phys.* **82** (4), 3045–3067.
- Heikkilä, T T, R. Ojajärvi, I. Maasilta, F. Giazotto, and F. S. Bergeret (2017), "Thermoelectric radiation detector based on superconductor/ferromagnet systems," arXiv:1709.08856.
- Higgs, Peter W (1964), "Broken symmetries and the masses of gauge bosons," *Phys. Rev. Lett.* **13**, 508–509.
- Hikino, Shin-ichi, Michiyasu Mori, Saburo Takahashi, and Sadamichi Maekawa (2011), "Composite excitation of Josephson phase and spin waves in Josephson junctions with ferromagnetic insulator," *J. Phys. Soc. Jpn* **80** (7), 074707.
- Hoffman, Silas, Koji Sato, and Yaroslav Tserkovnyak (2013), "Landau-Lifshitz theory of the longitudinal spin Seebeck effect," *Phys. Rev. B* **88**, 064408.
- Holmqvist, C, M. Fogelström, and W. Belzig (2014), "Spin-polarized Shapiro steps and spin-precession-assisted multiple Andreev reflection," *Phys. Rev. B* **90**, 014516.
- Holmqvist, C, S. Teber, and M. Fogelström (2011), "Nonequilibrium effects in a Josephson junction coupled to a precessing spin," *Phys. Rev. B* **83**, 104521.
- Houzert, Manuel (2008), "Ferromagnetic Josephson junction with precessing magnetization," *Phys. Rev. Lett.* **101**, 057009.
- Hübler, F, J C Lemyre, D Beckmann, and H v. Löhneysen (2010), "Charge imbalance in superconductors in the low-temperature limit," *Phys. Rev. B* **81** (18), 184524.
- Hübler, F, M. J. Wolf, D. Beckmann, and H. v. Löhneysen (2012), "Long-range spin-polarized quasiparticle transport in mesoscopic Al superconductors with a Zeeman splitting," *Phys. Rev. Lett.* **109** (20), 207001.
- Huertas-Hernando, Daniel, Yu. V. Nazarov, and W. Belzig (2002), "Absolute spin-valve effect with superconducting proximity structures," *Phys. Rev. Lett.* **88**, 047003.
- Hwang, Sun-Yong, Rosa López, and David Sánchez (2016), "Large thermoelectric power and figure of merit in a ferromagnetic-quantum dot-superconducting device," *Phys. Rev. B* **94**, 054506.
- Ivlev, B I, S. G. Lisitsyn, and G. M. Eliashberg (1973), "Nonequilibrium excitations in superconductors in high-frequency fields," *J. Low Temp. Phys.* **10** (3), 449–468.
- Izyumov, Yu A, Yu. N. Proshin, and M. G. Khusainov (2002), "Competition between superconductivity and magnetism in ferromagnet/superconductor heterostructures," *Phys. Usp.* **45**, 109–148.
- Jacquod, Philippe, Robert S. Whitney, Jonathan Meair, and Markus Büttiker (2012), "Onsager relations in coupled electric, thermoelectric, and spin transport: The tenfold way," *Phys. Rev. B* **86**, 155118.
- Jedema, F J, A T Filip, and B J van Wees (2001), "Electrical spin injection and accumulation at room temperature in an all-metal mesoscopic spin valve," *Nature* **410**, 345.
- Jedema, F J, H. B. Heersche, A. T. Filip, J. J. A. Baselmans, and B. J. van Wees (2002), "Electrical detection of spin precession in a metallic mesoscopic spin valve," *Nature* **416**, 713.
- Jedema, F J, M. S. Nijboer, A. T. Filip, and B. J. Van Wees (2003), "Spin injection and spin accumulation in all-metal mesoscopic spin valves," *Phys. Rev. B* **67** (8), 085319.
- Jiang, JS, Dragomir Davidović, Daniel H Reich, and CL Chien (1996), "Superconducting transition in nb/gd/nb trilayers," *Physical Review B* **54** (9), 6119.
- Johnson, Mark (1994), "Spin coupled resistance observed in ferromagnet-superconductor-ferromagnet trilayers," *Appl. Phys. Lett.* **65** (11), 1460–1462.
- Johnson, Mark, and R. H. Silsbee (1985), "Interfacial charge-spin coupling: Injection and detection of spin magnetization in metals," *Phys. Rev. Lett.* **55**, 1790–1793.

- Kalenkov, M S, A. D. Zaikin, and L. S. Kuzmin (2012), “Theory of a large thermoelectric effect in superconductors doped with magnetic impurities,” *Phys. Rev. Lett.* **109**, 147004.
- Kamenev, A, and A. Levchenko (2009), “Keldysh technique and non-linear  $\sigma$ -model: basic principles and applications,” *Adv. Phys.* **58**, 197.
- Kaplan, S B, C. C. Chi, D. N. Langenberg, J. J. Chang, S. Jafarey, and D. J. Scalapino (1976), “Quasiparticle and phonon lifetimes in superconductors,” *Phys. Rev. B* **14**, 4854–4873.
- Khusainov, M G (1996), “Indirect RKKY exchange and magnetic states of ferromagnet-superconductor superlattices,” *Zh. Eksp. Teor. Fiz.* **109** (2), 524, [*JETP* **82** (2), 278 (1996)].
- Kim, Sang Il, Kyu Hyoung Lee, Hyeon A Mun, Hyun Sik Kim, Sung Woo Hwang, Jong Wook Roh, Dae Jin Yang, Weon Ho Shin, Xiang Shu Li, Young Hee Lee, G. Jeffrey Snyder, and Sung Wng Kim (2015), “Dense dislocation arrays embedded in grain boundaries for high-performance bulk thermoelectrics,” *Science* **348** (6230), 109–114.
- Kivelson, S A, and D. S. Rokhsar (1990), “Bogoliubov quasiparticles, spinons, and spin-charge decoupling in superconductors,” *Phys. Rev. B* **41** (16), 11693–11696.
- Klapwijk, T M, J. N. Van den Bergh, and J. E. Mooij (1977), “Radiation-stimulated superconductivity,” *J. Low Temp. Phys.* **26** (3-4), 385–405.
- Kolenda, S, C. Sürgers, G. Fischer, and D. Beckmann (2017), “Thermoelectric effects in superconductor-ferromagnet tunnel junctions on europium sulfide,” *Phys. Rev. B* **95**, 224505.
- Kolenda, S, M. J. Wolf, and D. Beckmann (2016), “Observation of thermoelectric currents in high-field superconductor-ferromagnet tunnel junctions,” *Phys. Rev. Lett.* **116**, 097001.
- Konschelle, François, Ilya V Tokatly, and F Sebastián Bergéret (2015), “Theory of the spin-galvanic effect and the anomalous phase shift  $\varphi_0$  in superconductors and Josephson junctions with intrinsic spin-orbit coupling,” *Phys. Rev. B* **92** (12), 125443.
- Kontos, T, M Aprili, J Lesueur, and X Grison (2001), “Inhomogeneous superconductivity induced in a ferromagnet by proximity effect,” *Phys. Rev. Lett.* **86** (2), 304.
- Kopnin, N B (2001), *Theory of nonequilibrium superconductivity*, International series of monographs on physics No. 110 (Oxford University Press).
- Krishtop, Tatiana, Manuel Houzet, and Julia S. Meyer (2015), “Nonequilibrium spin transport in Zeeman-split superconductors,” *Phys. Rev. B* **91**, 121407.
- Kulagina, Iryna, and Jacob Linder (2014), “Spin supercurrent, magnetization dynamics, and  $\varphi$ -state in spin-textured Josephson junctions,” *Phys. Rev. B* **90**, 054504.
- Kupriyanov, M Yu, and V. F. Lukichev (1988), “Influence of boundary transparency on the critical current of “dirty” SS’S structures,” *Sov. Phys. JETP* **67** (6), 1163–1168.
- Lambert, C J, R. Raimondi, V. Sweeney, and A. F. Volkov (1997), “Boundary conditions for quasiclassical equations in the theory of superconductivity,” *Phys. Rev. B* **55**, 6015–6021.
- Langenberg, D N, and A. I. Larkin (1986), *Nonequilibrium superconductivity* (North-Holland, Amsterdam).
- Larkin, A I, and Yuri N. Ovchinnikov (1965), “Inhomogeneous state of superconductors,” *Sov. Phys. JETP* **20**, 762–769.
- Leivo, M M, J. P. Pekola, and D. V. Averin (1996), “Efficient Peltier refrigeration by a pair of normal metal/insulator/superconductor junctions,” *Appl. Phys. Lett.* **68** (14), 1996–1998.
- Linder, Jacob, and Marianne Etzelmüller Bathen (2016), “Spin caloritronics with superconductors: Enhanced thermoelectric effects, generalized Onsager response-matrix, and thermal spin currents,” *Phys. Rev. B* **93**, 224509.
- Linder, Jacob, Arne Brataas, Zahra Shomali, and Malek Zareyan (2012), “Spin-transfer and exchange torques in ferromagnetic superconductors,” *Phys. Rev. Lett.* **109**, 237206.
- Linder, Jacob, and Jason W. A. Robinson (2015), “Superconducting spintronics,” *Nat. Phys.* **11** (4), 307–315.
- Machon, P, M. Eschrig, and W. Belzig (2013), “Nonlocal thermoelectric effects and nonlocal Onsager relations in a three-terminal proximity-coupled superconductor-ferromagnet device,” *Phys. Rev. Lett.* **110** (4), 047002.
- Machon, P, M Eschrig, and W Belzig (2014), “Giant thermoelectric effects in a proximity-coupled superconductor-ferromagnet device,” *New. J. Phys.* **16** (7), 073002.
- Mai, S, E. Kandelaki, A. F. Volkov, and K. B. Efetov (2011), “Interaction of Josephson and magnetic oscillations in Josephson tunnel junctions with a ferromagnetic layer,” *Phys. Rev. B* **84**, 144519.
- Maki, K (1966), “Effect of Pauli paramagnetism on magnetic properties of high-field superconductors,” *Phys. Rev.* **148** (1), 362.
- Maki, K (1973), “Theory of electron-spin resonance in gapless superconductors,” *Phys. Rev. B* **8**, 191–199.
- Marchegiani, G, P. Virtanen, F. Giazotto, and M. Campisi (2016), “Self-oscillating Josephson quantum heat engine,” *Phys. Rev. Applied* **6**, 054014.
- Meissner, W Z (1927), “Das elektrische Verhalten der Metalle im Temperaturgebiet des flüssigen Heliums,” *Z. ges. Kälte-Industrie* **34**, 197.
- Menges, Fabian, Philipp Mensch, Heinz Schmid, Heike Riel, Andreas Stemmer, and Bernd Gotsmann (2016), “Temperature mapping of operating nanoscale devices by scanning probe thermometry,” *Nat. Commun.* **7**, 10874.
- Meservey, R, D. Paraskevopoulos, and P. M. Tedrow (1980), “Tunneling measurements of conduction-electron-spin polarization in heavy rare-earth metals,” *Phys. Rev. B* **22**, 1331–1337.
- Meservey, R, P. M. Tedrow, and Ronald C Bruno (1975), “Tunneling measurements on spin-paired superconductors with spin-orbit scattering,” *Phys. Rev. B* **11** (11), 4224.
- Meservey, R, P. M. Tedrow, and Peter Fulde (1970), “Magnetic field splitting of the quasiparticle states in superconducting aluminum films,” *Phys. Rev. Lett.* **25**, 1270–1272.
- Meservey, Robert, and P. M. Tedrow (1994), “Spin-polarized electron tunneling,” *Phys. Rep.* **238** (4), 173–243.
- Moodera, J S, X. Hao, G. A. Gibson, and R. Meservey (1988), “Electron-spin polarization in tunnel junctions in zero applied field with ferromagnetic EuS barriers,” *Phys. Rev. Lett.* **61**, 637–640.
- Moodera, J S, R. Meservey, and X. Hao (1993), “Variation of the electron-spin polarization in EuSe tunnel junctions from zero to near 100% in a magnetic field,” *Phys. Rev. Lett.* **70**, 853–856.
- Moodera, Jagadeesh S, Tiffany S Santos, and Taro Nagahama (2007), “The phenomena of spin-filter tunnelling,” *J. Phys.: Condens. Matter* **19** (16), 165202.

- Moodera, Jagadeesh Subbiah, Lisa R Kinder, Terrilyn M Wong, and R Meservey (1995), “Large magnetoresistance at room temperature in ferromagnetic thin film tunnel junctions,” *Physical review letters* **74** (16), 3273.
- Morten, J P, A. Brataas, and W. Belzig (2004), “Spin transport in diffusive superconductors,” *Phys. Rev. B* **70** (21), 212508.
- Morten, Jan Petter, Arne Brataas, and Wolfgang Belzig (2005), “Spin transport and magnetoresistance in ferromagnet/superconductor/ferromagnet spin valves,” *Phys. Rev. B* **72** (1), 014510.
- Münzenberg, M, and JS Moodera (2004), “Superconductor-ferromagnet tunneling measurements indicates p-spin and d-spin currents,” *Phys. Rev. B* **70** (6), 060402.
- Nagaosa, N, and Y. Tokura (2012), “Topological properties and dynamics of magnetic skyrmions,” *Nat. Nano* **8**, 899–911.
- Nahum, M, T. M. Eiles, and John M. Martinis (1994), “Electronic microrefrigerator based on a normal-insulator-superconductor tunnel junction,” *Appl. Phys. Lett.* **65** (24), 3123–3125.
- Narozhny, B N, I. L. Aleiner, and B. L. Altshuler (1999), “Theory of interaction effects in normal-metal-superconductor junctions out of equilibrium,” *Phys. Rev. B* **60** (10), 7213–7227.
- Nayak, Chetan, Steven H. Simon, Ady Stern, Michael Freedman, and Sankar Das Sarma (2008), “Non-Abelian anyons and topological quantum computation,” *Rev. Mod. Phys.* **80**, 1083–1159.
- Nazarov, Yu V (1999), “Novel circuit theory of Andreev reflection,” *Superlatt. Microstruct.* **25** (5-6), 1221–1231.
- Nemes, N M, J. E. Fischer, G. Baumgartner, L. Forró, T. Fehér, G. Oszlányi, F. Simon, and A. Jánosy (2000), “Conduction-electron spin resonance in the superconductor  $k_3C_{60}$ ,” *Phys. Rev. B* **61**, 7118–7121.
- Nielsen, J Beyer, C. J. Pethick, J Rammer, and H Smith (1982), “Pair breaking and charge relaxation in superconductors,” *J. Low Temp. Phys.* **46** (5-6), 565–597.
- Onsager, Lars (1931), “Reciprocal relations in irreversible processes. I.” *Phys. Rev.* **37**, 405–426.
- Ozaeta, A, P. Virtanen, F. S. Bergeret, and T. T. Heikkilä (2014), “Predicted very large thermoelectric effect in ferromagnet-superconductor junctions in the presence of a spin-splitting magnetic field,” *Phys. Rev. Lett.* **112** (5), 057001.
- Pal, Avradeep, and M. G. Blamire (2015), “Large interfacial exchange fields in a thick superconducting film coupled to a spin-filter tunnel barrier,” *Phys. Rev. B* **92**, 180510.
- Paraskevopoulos, D, R. Meservey, and P. M. Tedrow (1977), “Spin polarization of electrons tunneling from 3d ferromagnetic metals and alloys,” *Phys. Rev. B* **16**, 4907–4919.
- Pekola, J P, T. T. Heikkilä, A. M. Savin, J. T. Flyktman, F. Giazotto, and F. W. J. Hekking (2004), “Limitations in cooling electrons using normal-metal-superconductor tunnel junctions,” *Phys. Rev. Lett.* **92**, 056804.
- Pershoguba, S S, K. Björnson, A. M. Black-Schaffer, and A. V. Balatsky (2015), “Currents induced by magnetic impurities in superconductors with spin-orbit coupling,” *Phys. Rev. Lett.* **115**, 116602.
- Poli, Ninos, Jan Petter Morten, Mattias Urech, Arne Brataas, David B Haviland, and Vladislav Korenivski (2008), “Spin injection and relaxation in a mesoscopic superconductor,” *Phys. Rev. Lett.* **100** (13), 136601.
- Qi, Xiao-Liang, and Shou-Cheng Zhang (2011), “Topological insulators and superconductors,” *Rev. Mod. Phys.* **83** (4), 1057–1110.
- Quay, C H L, and M. Aprili (2017), “Out-of-equilibrium spin transport in mesoscopic superconductors,” arXiv:arXiv:1705.07770.
- Quay, C H L, D. Chevallier, C. Bena, and M. Aprili (2013), “Spin imbalance and spin-charge separation in a mesoscopic superconductor,” *Nat. Phys.* **9** (2), 84–88.
- Quay, C H L, Y. Chiffaudel, C. Strunk, and M. Aprili (2015), “Quasiparticle spin resonance and coherence in superconducting aluminium,” *Nat. Commun.* **6**, 8660.
- Quay, C H L, C. Dutreix, D. Chevallier, C. Bena, and M. Aprili (2016), “Frequency-domain measurement of the spin-imbalance lifetime in superconductors,” *Phys. Rev. B* **93**, 220501.
- Rezaei, Ali, Akashdeep Kamra, Peter Machon, and Wolfgang Belzig (2017), “Spin-flip enhanced thermoelectricity in superconductor-ferromagnet bilayers,” arXiv preprint arXiv:1711.11538.
- Richard, Caroline, Manuel Houzet, and Julia S. Meyer (2012), “Andreev current induced by ferromagnetic resonance,” *Phys. Rev. Lett.* **109**, 057002.
- Rouco, Mikel, Tero T Heikkilä, and F Sebastian Bergeret (2018), “Electron refrigeration in hybrid structures with spin-split superconductors,” *Physical Review B* **97** (1), 014529.
- Ryazanov, V V, V. A. Oboznov, A. Yu. Rusanov, A. V. Veretennikov, A. A. Golubov, and J. Aarts (2001), “Coupling of two superconductors through a ferromagnet: evidence for a  $\pi$  junction,” *Phys. Rev. Lett.* **86** (11), 2427.
- Saint-James, D, G. Sarma, and E.J. Thomas (1969), *Type II Superconductivity*, Commonwealth and International Library. Liberal Studies Divi (Elsevier Science & Technology).
- Schmid, Albert, and Gerd Schön (1975), “Linearized kinetic equations and relaxation processes of a superconductor near  $T_c$ ,” *J. Low Temp. Phys.* **20** (1), 207–227.
- Senapati, Kartik, Mark G. Blamire, and Zoe H. Barber (2011), “Spin-filter Josephson junctions,” *Nat. Mater* **10** (11), 849–852.
- Serene, J W, and D. Rainer (1983), “The quasiclassical approach to superfluid  $^3He$ ,” *Phys. Rep.* **101**, 221.
- Shelly, Connor D, Ekaterina A. Matrozova, and Victor T. Petrashov (2016), “Resolving thermoelectric “paradox” in superconductors,” *Sci. Adv.* **2** (2), e1501250.
- Shin, Y-S, H.-J. Lee, and H.-W. Lee (2005), “Spin relaxation in mesoscopic superconducting Al wires,” *Phys. Rev. B* **71**, 144513.
- Silaev, Mihail, P Virtanen, F. S. Bergeret, and T. T. Heikkilä (2015a), “Long-range spin accumulation from heat injection in mesoscopic superconductors with Zeeman splitting,” *Phys. Rev. Lett.* **114** (16), 167002.
- Silaev, Mihail, P Virtanen, T. T. Heikkilä, and F. S. Bergeret (2015b), “Spin Hanle effect in mesoscopic superconductors,” *Phys. Rev. B* **91** (2), 024506.
- Singh, A, S. Voltan, K. Lahabi, and J. Aarts (2015), “Colossal proximity effect in a superconducting triplet spin valve based on the half-metallic ferromagnet  $CrO_2$ ,” *Phys. Rev. X* **5**, 021019.
- Singh, Amrita, Charlotte Jansen, Kaveh Lahabi, and Jan Aarts (2016), “High-quality  $CrO_2$  nanowires for dissipationless spintronics,” *Phys. Rev. X* **6** (4), 041012.



- Skadsem, Hans Joakim, Arne Brataas, Jan Martinek, and Yaroslav Tserkovnyak (2011), “Ferromagnetic resonance and voltage-induced transport in normal metal-ferromagnet-superconductor trilayers,” *Phys. Rev. B* **84**, 104420.
- Snyder, G Jeffrey, and Tristan S. Ursell (2003), “Thermoelectric efficiency and compatibility,” *Phys. Rev. Lett.* **91**, 148301.
- van Son, P C, H. van Kempen, and P. Wyder (1987), “Boundary resistance of the ferromagnetic-nonferromagnetic metal interface,” *Phys. Rev. Lett.* **58**, 2271–2273.
- Soumyanarayanan, A, N. Reyren, A. Fert, and C. Panagopoulos (2016), “Emergent phenomena induced by spin-orbit coupling at surfaces and interfaces,” *Nature* **539**, 509–517.
- Strambini, E, F. S. Bergeret, and F. Giazotto (2015), “Mesoscopic Josephson junctions with switchable current-phase relation,” *EPL* **112** (1), 17013.
- Strambini, E, V. N. Golovach, G. De Simoni, J. S. Mooder, F. S. Bergeret, and F. Giazotto (2017), “Revealing the magnetic proximity effect in eus/al bilayers through superconducting tunneling spectroscopy,” *Phys. Rev. Materials* **1** (5), 054402.
- Takahashi, S, and S. Maekawa (2003), “Spin injection and detection in magnetic nanostructures,” *Phys. Rev. B* **67** (5), 052409.
- Tedrow, P M, and R. Meservey (1971), “Spin-dependent tunneling into ferromagnetic nickel,” *Phys. Rev. Lett.* **26**, 192–195.
- Tedrow, P M, and R. Meservey (1973), “Spin polarization of electrons tunneling from films of Fe, Co, Ni, and Gd,” *Phys. Rev. B* **7** (1), 318.
- Tedrow, P M, J. E. Tkaczyk, and A. Kumar (1986), “Spin-polarized electron tunneling study of an artificially layered superconductor with internal magnetic field: EuO-Al,” *Phys. Rev. Lett.* **56**, 1746–1749.
- Tinkham, M (1972), “Tunneling generation, relaxation, and tunneling detection of hole-electron imbalance in superconductors,” *Phys. Rev. B* **6**, 1747–1756.
- Tinkham, M, and John Clarke (1972), “Theory of pair-quasiparticle potential difference in nonequilibrium superconductors,” *Phys. Rev. Lett.* **28**, 1366–1369.
- Tinkham, Michael (1996), *Introduction to superconductivity* (Courier Corporation).
- Tokuyasu, T, J. A. Sauls, and D. Rainer (1988), “Proximity effect of a ferromagnetic insulator in contact with a superconductor,” *Phys. Rev. B* **38**, 8823–8833.
- Torrey, H C (1956), “Bloch equations with diffusion terms,” *Phys. Rev.* **104**, 563–565.
- Trif, Mircea, and Yaroslav Tserkovnyak (2013), “Dynamic magnetoelectric effect in ferromagnet/superconductor tunnel junctions,” *Phys. Rev. Lett.* **111**, 087602.
- Tserkovnyak, Yaroslav, Arne Brataas, Gerrit E. W. Bauer, and Bertrand I. Halperin (2005), “Nonlocal magnetization dynamics in ferromagnetic heterostructures,” *Rev. Mod. Phys.* **77**, 1375–1421.
- Uchida, K, M. Ishida, T. Kikkawa, A. Kirihara, T. Murakami, and E. Saitoh (2014), “Longitudinal spin Seebeck effect: from fundamentals to applications,” *J. Phys.: Condens. Matter* **26** (34), 343202.
- Usadel, Klaus D (1970), “Generalized diffusion equation for superconducting alloys,” *Phys. Rev. Lett.* **25** (8), 507–509.
- Van Harlingen, D J, D. F. Heidel, and J. C. Garland (1980), “Experimental study of thermoelectricity in superconducting indium,” *Phys. Rev. B* **21**, 1842–1857.
- Vier, D C, and S. Schultz (1983), “Observation of conduction electron spin resonance in both the normal and superconducting states of niobium,” *Phys. Lett. A* **98**, 283.
- Villamor, Estitxu, Miren Isasa, Saül Vélez, Amilcar Bedoya-Pinto, Paolo Vavassori, Luis E. Hueso, F. Sebastián Bergeret, and Fèlix Casanova (2015), “Modulation of pure spin currents with a ferromagnetic insulator,” *Phys. Rev. B* **91** (2), 020403.
- Virtanen, P, T. T. Heikkilä, and F. S. Bergeret (2016), “Stimulated quasiparticles in spin-split superconductors,” *Phys. Rev. B* **93** (1), 014512.
- Waintal, Xavier, and Piet W. Brouwer (2002), “Magnetic exchange interaction induced by a Josephson current,” *Phys. Rev. B* **65**, 054407.
- Wakamura, T, N Hasegawa, K Ohnishi, Y Niimi, and YoshiChika Otani (2014), “Spin injection into a superconductor with strong spin-orbit coupling,” *Phys. Rev. Lett.* **112** (3), 036602.
- Wellstood, F C, C. Urbina, and John Clarke (1994), “Hot-electron effects in metals,” *Phys. Rev. B* **49**, 5942–5955.
- Wolf, M J, F Hübner, S Kolenda, and D Beckmann (2014a), “Charge and spin transport in mesoscopic superconductors,” *Beilstein J. Nanotech.* **5** (1), 180–185.
- Wolf, M J, F. Hübner, S. Kolenda, H. v. Löhneysen, and D. Beckmann (2013), “Spin injection from a normal metal into a mesoscopic superconductor,” *Phys. Rev. B* **87**, 024517.
- Wolf, M J, C. Sürgers, G Fischer, and D Beckmann (2014b), “Spin-polarized quasiparticle transport in exchange-split superconducting aluminum on europium sulfide,” *Phys. Rev. B* **90**, 144509.
- Xiong, Y M, S. Stadler, P. W. Adams, and G. Catelani (2011), “Spin-resolved tunneling studies of the exchange field in EuS/Al bilayers,” *Phys. Rev. Lett.* **106**, 247001.
- Yafet, Y, D. C. Vier, and S. Schultz (1984), “Conduction electron spin resonance and relaxation in the superconducting state,” *J. Appl. Phys.* **55** (6), 2022–2024.
- Yagi, Ryuta (2006), “Charge imbalance observed in voltage-biased superconductor-normal tunnel junctions,” *Phys. Rev. B* **73** (13), 134507.
- Yang, Hyunsoo, See-Hun Yang, Saburo Takahashi, Sadamichi Maekawa, and Stuart S. P. Parkin (2010), “Extremely long quasiparticle spin lifetimes in superconducting aluminium using MgO tunnel spin injectors,” *Nat. Mater.* **9** (7), 586–593.
- Yang, Tao, Takashi Kimura, and Yoshichika Otani (2008), “Giant spin-accumulation signal and pure spin-current-induced reversible magnetization switching,” *Nat. Phys.* **4** (11), 851–854.
- Yosida, Kei (1958), “Paramagnetic susceptibility in superconductors,” *Phys. Rev.* **110** (3), 769.
- Zaitsev, A V (1984), “Quasiclassical equations of the theory of superconductivity for contiguous metals and the properties of constricted microcontacts,” *Sov. Phys. JETP* **59** (5), 1015.
- Zhao, Erhai, Tomas Löfwander, and J. A. Sauls (2004), “Nonequilibrium superconductivity near spin-active interfaces,” *Phys. Rev. B* **70**, 134510.
- Zhao, Hui Lin, and Selman Hershfield (1995), “Tunneling, relaxation of spin-polarized quasiparticles, and spin-charge separation in superconductors,” *Phys. Rev. B* **52**, 3632–3638.

Zhao, Li-Dong, Gangjian Tan, Shiqiang Hao, Jiaqing He, Yanling Pei, Hang Chi, Heng Wang, Shengkai Gong, Huibin Xu, Vinayak P. Dravid, Ctirad Uher, G. Jeffrey Snyder, Chris Wolverton, and Mercouri G. Kanatzidis (2016), “Ul-

trahigh power factor and thermoelectric performance in hole-doped single-crystal SnSe,” *Science* **351** (6269), 141–144.